Orientation selectivity in the population of ON-OFF direction-selective ganglion cells in the mouse retina

by

Prathyusha Ravi Chander

B.E., Anna University, 2017

A Thesis Submitted in Partial

Fulfillment of the Requirements for

the Degree of

MASTER OF SCIENCE

In the Department of Biology

University of Victoria

Supervisory Committee

Orientation selectivity across the population of ON-OFF direction-selective ganglion cells in the mouse retina

by

Prathyusha Ravi Chander

B.E., Anna University, 2017

Supervisory Committee

Dr. Gautam B. Awatramani, Department of Biology

Supervisor

Dr. Kerry R. Delaney, Department of Biology

Committee Member

Dr. Robert L. Chow, Department of Biology

Committee Member

Abstract

In the mammalian retina, the orientation-selective (OS) and direction-selective (DS) information are generally thought to be relayed to higher visual centers via distinct ganglion cell types. Contrary to this notion, here I report that classic ON-OFF direction-selective ganglion cells (DSGCs) that are known to encode the four cardinal directions, also encode orientation of static stimuli. The DSGC's preferred orientations was always orthogonal to its preferred-null axis defined by moving stimuli. To evaluate the synaptic mechanisms underlying orientation selectivity a combination of electrophysiological, optogenetic, and gene knock-out techniques were used to assess the functional properties of all four types of ON-OFF DSGCs. Cumulative results from multiple approaches revealed that the glutamate input to all four types of DSGCs was tuned to the vertical axis. This relies on signals from a specific presynaptic source (the bipolar cell type 5A; BC5A), which appear to be electrically coupled to vertically oriented processes of wide-field amacrine cells. By contrast, the GABAergic inhibition mediated largely by starburst amacrine cells was tuned either along the horizontal or vertical axis, consistent with their well-defined asymmetric wiring pattern. Thus, distinct combinations of inhibition and excitation underlie orientation selectivity in the nasal/temporal and dorsal/ventral coding DSGC populations, only the latter critically relying on the starbursts. Together, my work provides novel insights into how feature selectivity emerges in the hierarchical network in the retina.

Table of Contents

Highlights

a. All 4 types of ON-OFF DSGCs have an orientation selectivity that is orthogonal to the preferred direction of motion.
b. Strength of the orientation selectivity observed in ON-OFF DSGCs is stable across different contrast levels.
c. Robust orientation selectivity is observed when inhibitory mechanisms driving the direction selectivity in the circuit are blocked.
d. Asymmetric distal excitation is tuned for vertical orientation.
e. Optogenetic stimulation of bipolar cells type 5A or 5i (BC5A) using channelrhodopsin (ChR2) reveals distal excitation that is tuned to the dorso-ventral axis of the retina.
f. Orientation tuning of ON-OFF DSGCs rely on connexin 36-containing gap junctions.
g. Strong tuning in the OFF responses confirm the ON specificity of genetic manipulation in the connexin 36 knockout mouse model.
h. Surround glutamatergic excitation is absent when connexin 36 containing gap junctions are knocked out.
i. OS inhibition from starburst amacrine cells (SACs) is tuned to the P-N axis of the ON-OFF DSGCs.
j. Asymmetric GABAergic inhibition from SACs and symmetric glutamatergic excitation from BC5As contribute to orientation selectivity in D/V (I competes against E) vs N/T (E/I are complementary) coding ON-OFF DSGCs.

List of Figures

List of Abbreviations

AC	Amacrine cell
ACh	Acetylcholine
AMPA	α-amino-3-hydroxy-5-methyl-4-isoxazolepropionic acid
BC	Bipolar cell
BC5A	Bipolar cell type 5A
ChAT	Choline aceytltransferase
CNS	Central nervous system
Cx36	Connexin 36
DCG-IV	(1R,2R)-3-[(1S)-1-amino-2-hydroxy-2-oxoethyl] cyclopropane-1,2-dicarboxylic acid
DS	Direction-selective
DSGC	Direction-selective ganglion cell
DSI	Direction selectivity index
EPSC	Excitatory postsynaptic current
FWHM	Full-width half-maximum
GABA	γ-aminobutyric acid
GCL	Ganglion cell layer
GFP	Green fluorescent protein
GPCR	G-protein coupled receptor
HC	Horizontal cell
HEX	Hexamethonium
IPSC	Inhibitory postsynaptic current
INL	Inner nuclear layer
IPL	Inner plexiform layer
Kcng4	Potassium voltage-gated channel modifier subfamily G member 4
KO	Knockout
L-AP4	L-2-amino-4-phosphonobutyric acid
NMDA	N-methyl-D-aspartate
ONL	Outer nuclear layer
OPL	Outer plexiform layer
OS	Orientation-selective
OSGC	Orientation-selective ganglion cell
OSI	Orientation selectivity index
RPE	Retinal pigment epithelium
SAC	Starburst amacrine cell
SR	Gabazine
TPMPA	(1,2,5,6-Tetrahydropyridin-4-yl) methylphosphinic acid
TRHR	Thyrotropin releasing hormone receptor
UBP-310	(S)-1-(2-Amino-2-carboxyethyl)-3-(2-carboxy-thiophene-3-yl-methyl)-5-methylpyrimidine-2,4-dione
WT	Wild-type

Acknowledgements

I would like to thank my supervisor, Dr. Gautam B. Awatramani for his continuous support and mentorship throughout my graduate studies. Without him this work would not have been possible. I would like to thank all the past and present members of the Awatramani lab (incomplete and in no particular order) Dr. Santhosh Sethuramanujam, Dr. Varsha Jain, Dr. Benjamin Murphy-Baum and Dr. Prerna Srivastava, Dr. Laura Hanson, Tracy Michaels, Geoff deRosenroll, Pavitra Chundekkad, Ilya Capralov, Gemma Graham, Aven Cosby, Jerram Gawley for all their support and encouragement. I would like to extend my gratitude especially to Dr. Laura Hanson and Dr. Benjamin Murphy-Baum, and Dr. Prerna Srivastava for their input and guidance with the techniques, experimental design, and data analysis as well as Tracy Michaels for all the mouse colony work.

I would like to thank my supervisory committee, Dr. Robert L. Chow and Dr. Kerry R. Delaney, for their continuous support throughout this project.

Finally, I would also like to thank all of the wonderful people I've befriended over the past few years, who have made me feel secure and at home in a new country. Starting off this journey in a new country, especially during the pandemic was very challenging, and I would have been lost if not for all the support from my friends and family all throughout.

1. Introduction

The mouse retina is an organized and layered structure with genetic-defined components and thus provides an excellent system for studying the hierarchical processing of visual information. Classic single-unit recordings have shown that orientation and direction are encoded by distinct orientation- and direction-selective ganglion cells (OSGCs and DSGCs, respectively), which relay information to higher visual areas. Since then, OSGCs and DSGCs have been identified in the retinas of most species examined including rodents and primates (Passaglia et al., 2002; Levick, 1967; Caldwell & Daw, 1978; Bloomfield 1994; Venkataramani & Taylor, 2010, 2016; Murphy-Baum & Taylor 2015; Nath & Schwartz, 2016, 2017). How these features are extracted by different layers of the retina is an area of active investigation.

1.1 Structure and Function of the Retina

The retina lies at the back of the eye and contains millions of photoreceptors (i.e., rods and cones) that convert light information received from the outside world into a series of spiking electrical signals, relying on specific opsin molecules. Cone opsins and rhodopsins present in the photoreceptors are G-protein-coupled receptors (GPCRs) that convert light into electrochemical signals which produce hyperpolarization of the photoreceptors. This process of phototransduction takes place in specialized cellular compartments in the outer segments that are surrounded by retinal pigment epithelium (RPE) cells (Koch and Dell'Orco, 2015). Photoreceptors utilize ribbon synapses to respond to changes in light intensity in a graded fashion (Raviola and Gilula, 1973; Heidelberger, Thoreson and Witkovsky, 2005). Physiological responses measured from these photoreceptors have shown that these cells are active in the dark and release the neurotransmitter glutamate to the synaptic cleft whereas light-induced

hyperpolarization stops the glutamate secretion. The glutamate released from these cells invokes activity in the postsynaptic bipolar and horizontal cells (HC) (Heidelberger et al., 2005), thereby transmitting the sensory light information to a secondary layer of neurons. Photoreceptors exhibit high degrees of electrical coupling with their post-synaptic partners through gap-junctions, which are modulated by varying background light intensities (Bloomfield and Völgyi, 2009; Roy and Field, 2019).

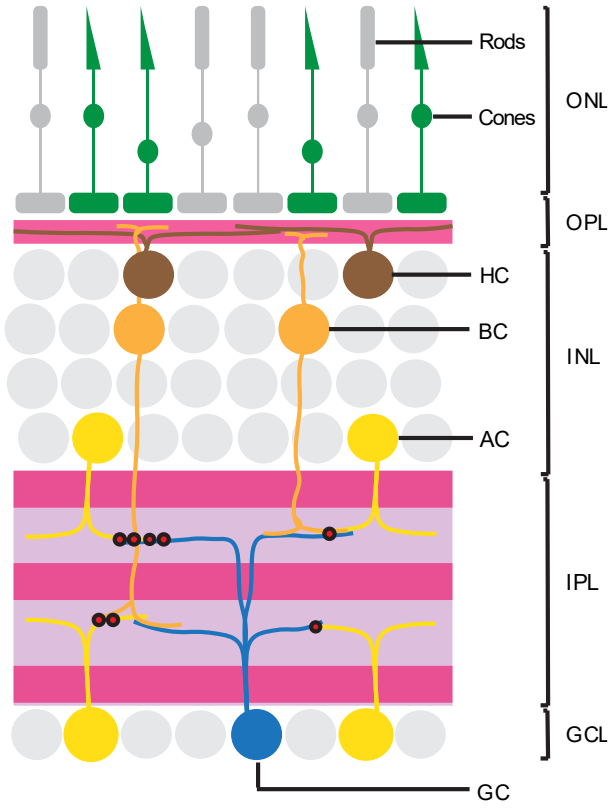

Figure 1.1 Schematic of the retinal circuitry

Light incident on the eyes is first detected by the photoreceptors (rods and cones) in the ONL of the retina. It is then passed on to the bipolar cells in the INL. Signal from the bipolar cells are modulated by the amacrine cells before it reaches the ganglion cells, which then take the information to the higher brain regions via their axons (optic nerve) for further processing (Dowling 1987). (OPL = outer plexiform layer, ONL – outer nuclear layer, INL = inner nuclear layer, IPL = inner plexiform layer, HC – horizontal cell, GCL = ganglion cell layer, BC – bipolar cell, AC – amacrine cell, GC – ganglion cell). Adapted from Liu and Sanes, 2014.

The outer plexiform layer (OPL) of the retina comprises the photoreceptor-bipolar cell synaptic connections, along with lateral connections from horizontal cells. The signals from these connections pass through two pathways, split between the two major classifications of bipolar cells: ON bipolar cells (which depolarize in response to light), and OFF bipolar cells (which hyperpolarize in response to light). These bipolar cells are further categorized into sustained, and transient types, each having various subtypes of their own (Kaneko, 1970; Werblin & Dowling, 1969; Nelson and Kolb, 1983, Kolb, 2003). In the mouse retina, there is a total of ~15 bipolar cell subtypes, each of which projects to a specific sub-lamina in the inner plexiform layer (IPL), with ON BCs projecting more proximal to the ganglion cell layer and OFF BCs projecting distally (Famiglietti and Kolb, 1976). Similar to photoreceptors, bipolar cells utilize ribbon synapses to release glutamate in a graded fashion, which is in contrast to the action potential mediated all-or-none mechanism observed in most other neurons (Heidelberger, Thoreson and Witkovsky, 2005; Singer 2007; Rudolph et al., 2015).

The amacrine cells (AC) are the next set of interneurons found downstream to the bipolar cells, which further refine the visual signals. This tertiary block in the signal propagation cascade involves ~ 60 different types of genetically distinguishable amacrine cells which determine the properties of visual stimuli to which ganglion cells preferentially respond (Yan et al., 2020). It is predicted that 2-3 types of amacrine cells participate in shaping the response properties of each ganglion cell circuit (Masland, 2012). Each of these amacrine cells are morphologically diverse, have widespread connectivity, and distinct biophysical properties (activation). It is an important goal in the study of retinal circuitry to determine which amacrine cells are involved in the computation by which ganglion cell circuit, which stimuli drive activation of each amacrine cell, and under what physiological conditions are different amacrine cells activated.

Ganglion cells are the output neurons of the retina. They receive synaptic inputs from bipolar cells and amacrine cells and send action potentials down the optic nerve to higher sensory processing regions in the brain (Schiller, 2010; Masland, 2012). Ganglion cells can be categorized based on their morphology, physiological responses, or genetic markers (Koch et al., 1982; Sumbul et al., 2014, Li et al., 2015, Sanes and Masland, 2015). The functionalities of these ganglion cell populations rely on the presynaptic partners that facilitate specific feature extraction from the visual environment. Numerous ganglion cell circuits are involved in extracting specific features from the visual world, such as size, shape, direction, orientation, color, and contrast. Each of these ganglion cell types, along with their presynaptic bipolar and amacrine cells, work in tandem to carry the light information incident on the eyes to the higher brain centers for further processing and interpretation (Kolb et al., 1981; Rockhill et al., 2002; Dacey et al., 2004; Sanes et al., 2015). However, it is traditionally thought that individual ganglion cell types relay information about a single visual feature.

A major challenge faced when studying these retinal circuits includes identification of the cellular components of each of these circuits and understanding their functional properties. In order to better understand retinal network physiology, research over the past few decades has been focused on deciphering how a few ganglion cell types process information. To date, some of the best described circuits in the retina are the ones that encode stimulus direction and orientation. Researchers have been investigating the circuit elements encoding direction and orientation information from the visual scene for many decades and have shown that separate populations of ganglion cells relay DS and OS information to the higher brain regions. (Barlow and Levick, 1965; Borst and Euler, 2011; Vaney et al., 2012; Levick 1967; Nath & Schwartz, 2016). In a recent study we found that ON-OFF DSGCs encode both DS and OS information (Hanson et al., 2023). However, the synaptic mechanisms that enable all 4

types of ON-OFF DSGCs to mediate orientation selectivity remains to be discovered and is the main focus of my thesis.

1.2 Direction Selectivity in the Retina

The DS circuit in the retina is one of the most well studied neural circuits, at a physiological level (Barlow and hill., 1963, 1964; Barlow & Levick, 1965; Amthor et al. 1984; Oyster et al. 1972; Wyatt and Daw 1975; Yang and Masland 1992, 1994; Weng et al., 2005; Demb et al., 2007; Borst and Euler, 2011; Vaney et al., 2012; Sivyer 2013), and anatomical level (Briggman et al., 2011, Helmstaedter et al., 2013, Kim et al., 2014). Retinal DS appears to be conserved in numerous species (Thorson, 1964; Barlow and Levick, 1965; Borst and Euler, 2011) and in most cases is conveyed by two distinct specialized ganglion cell classes, namely ON and OFF DSGCs (Barlow and Levick, 1965; Borst and Euler, 2011; Vaney et al., 2012). ON-OFF DSGCs fire bursts of action potential as the leading and trailing edges of bright objects moving in a ‘preferred’ direction (PD) traverse their receptive fields but are silent when the same object moves in the opposite or ‘null’ direction (ND). (Taylor and Vaney, 2002; Vaney et al., 2012; Taylor and Smith, 2012). The PDs of ON-OFF DSGCs cluster along the four cardinal directions, are often referred to as dorsal- (or superior-), ventral- (or inferior-), temporal- (or anterior)-, and nasal- (or posterior)- coding DSGCs (Barlow & Levick, 1965; Oyster and Barlow, 1967, Yonehara et al., 2013). By contrast, ON DSGCs only respond to leading edge of bright objects, and their PDs appear to align with the orientation of the semicircular canals in the inner ear thus defining 3 types (Oyster et al., 1972, Dhande et al., 2013; however, (Sabah et al., 2021) suggested 4 types of ON DSGCs in mouse retina) similar to the ON-OFF DSGCs.

The major mechanism driving direction selectivity in the mouse retina involves asymmetric inhibitory synaptic input mediated by the starburst amacrine cell (SAC), resulting from an asymmetric wiring pattern (Fried et al., 2002; Lee et al., 2010; Briggman et al., 2011; Yonehara et al., 2013; Chen et al., 2016; Brombas et al., 2017).

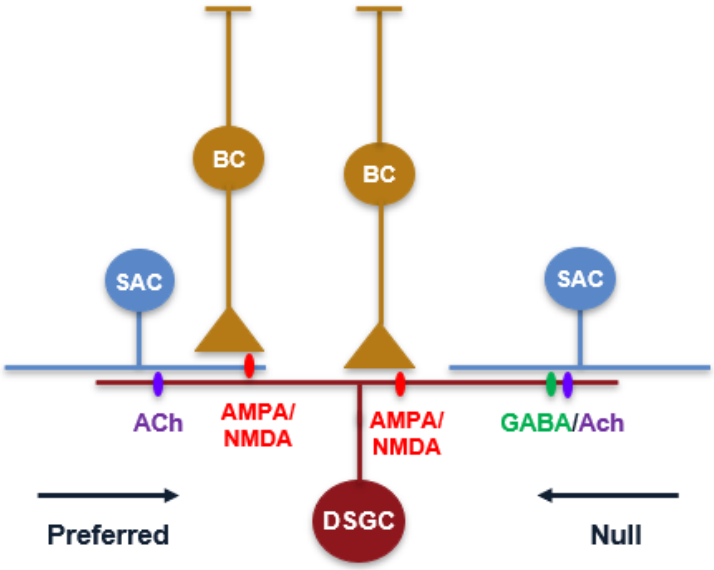

Figure 1.2 Mechanism of DS generation in ON-OFF DSGCs

A schematic of the functional circuitry underlying direction selectivity in ON-OFF DSGCs. These ON-OFF DSGC have two pre-synaptic partners, namely the SACs which provide cholinergic excitation (Preferred and Null directions) and GABAergic inhibition (Null) and glutamatergic bipolar cells (AMPA/NMDA). DSGC – Direction-selective ganglion cell; SAC – Starburst amacrine cell; Ach – Acetylcholine; AMPA – Alpha-amino-3-hydroxy-5-Methyl-4-isoxazole Propionic Acid; NMDA – N-Methyl-D-Aspartate; BC – Bipolar cells; GABA – Gamma-Amino Butyric Acid.

The main source of asymmetric GABAergic inhibition (Gamma-Amino Butyric Acid - an inhibitory neurotransmitter) is provided to DSGCs along the null direction by SACs via $GABA_A$ receptors. Distinct populations of ON and OFF SACs synapse on to the ON and OFF dendrites of

DSGCs in defined layers of the IPL (Famiglietti, 1983; O'Malley et al., 1992; Yoshida et al., 2001; Vlasits et al., 2014).

Starburst cells also co-release a second neurotransmitter: acetylcholine (ACh). DSGCs express nicotinic acetylcholine receptors (nAChRs) that mediate rapid excitatory responses (O'Malley and Masland, 1989; Lee et al., 2010; Pei et al., 2015; Taylor and Smith, 2012; Sethuramanujam et al., 2016; Brombas et al., 2017). Interestingly, unlike GABA, ACh appears to spread beyond the confines of the 'wrap-around' synapses observed between SACs and DSGCs, to have more widespread effect (Sethuramanujam et al., 2016). As a result, cholinergic excitation is symmetrical when averaged over the DSGC's dendritic tree.

In contrast to starburst GABA release, glutamatergic excitation provided by bipolar cells (BCs) is symmetrical (Yonehara et al., 2013; Park et al., 2014). BCs form specialized 'ribbon' synapses which enable continuous vesicle release (Heidelberger, Thoreson and Witkovsky, 2005; Singer 2007; Rudolph et al., 2015). These ribbons are often positioned across the junction of two-postsynaptic partners forming a 'dyad' synapse. Serial block electron microscopy (SBEM) analysis shows that an overlapping set of BCs drive SACs and DSGCs. Interestingly, glutamate responses in SAC are mediated mainly by AMPA receptors, while responses of DSGCs are mediated by NMDA receptors (Sethuramanujam et al., 2017).

There are also other parallel mechanisms for DS generation in the downstream ganglion cells, namely the ones involving temporal asymmetries between excitation and inhibition, provided by differential connectivity patterns of cholinergic and GABAergic SAC inputs to DSGCs (Hanson et al., 2019). In a DSGC, a temporal offset between the excitation and inhibition has been shown to be necessary to confer directionality to the downstream ganglion cells. In addition to this temporal delay, spatial asymmetry in the signal propagation from the SACs dendrites to the dendrites of the DSGCs has also been shown to be critical for generation of DS (Hanson et al., 2019).

Pharmacological manipulations and genetic knockout models have shown that DS is lost under conditions where the SAC outputs are abolished by using DCG-IV, an agonist for mGluR2,3 receptors (Sethuramanujam et al., 2016, Hanson et al., 2019, Hanson et al., 2023). The glutamatergic signals and calcium responses measured from the presynaptic BC terminals synapsing on to the dendrites of the DSGCs have been shown to be non-directional (Yonehara et al., 2013; Park et al., 2014; Sethuramanujam et al., 2016; Sethuramanujam et al., 2017). It is now well established that direction selectivity relies on the integration of non-directional glutamatergic signals mediated by a well-defined population of BCs, with directional GABAergic and cholinergic signals mediated by DS dendrites of SACs. Thus, all previous studies have implicated the critical role that starburst amacrine cells hold in conferring directionality to the downstream ganglion cells (Yonehara et al., 2013; Park et al., 2014; Sethuramanujam et al., 2016; Sethuramanujam et al., 2017).

Apart from these mechanisms, the starburst circuitry is also regulated by specific types of narrow-, medium- and wide-field amacrine cells (including the starbursts themselves) that enable the circuit to maintain its coding properties across a range of stimulus sizes and contrasts (Hoggarth et al., 2015; Ding et al., 2016; Wei wei et al., 2019; Jain et al., 2022).

In a tour de force study, Briggman et al., (2013) mapped out the anatomical connectivity between the starburst dendrites and four types of ON-OFF DSGCs that encode the cardinal directions and showing them to be in an anti-parallel configuration (Figure 1.3A-B). It is now well-accepted that this wiring specificity, along with the DS properties of starburst dendrites ensures that the excitatory/inhibitory drive to each type of DSGC is modulated in a DS manner resulting in directionally tuned spiking output patterns. A multitude of research from the past has highlighted the potential for manipulating different components involved in this DS circuitry and created an ideal platform to utilize the mouse retina as a base model for studying isolated circuit connections. For this thesis, I will use the

DS circuitry involving ON-OFF DSGCs and its presynaptic partners as a base model for studying how multiple features from the visual environment could potentially be conveyed through a single circuit pathway.

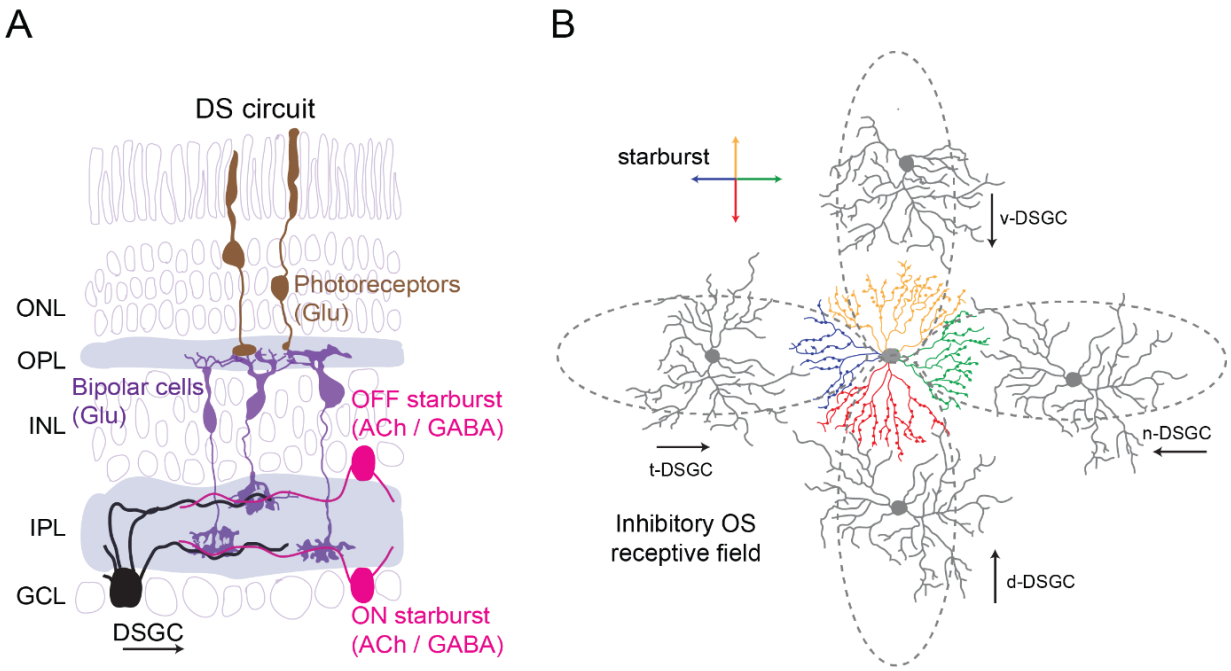

Figure 1.3 Schematic representation of the DS circuitry

(A) Schematic of DS circuitry showing ON-OFF DSGC and its presynaptic partner, null SACs (GABA only) and glutamatergic bipolar cells (AMPA/NMDA). (B) Schematic representation of null SAC connectivity with all 4 types of ON-OFF DSGCs providing inhibitory OS receptive field. Thus, the GABAergic/cholinergic signals mediated by starbursts are differentially transmitted to the DSGCs. (OPL = outer plexiform layer, INL = inner nuclear layer, IPL = inner plexiform layer which can be separated into the ON and OFF layers, GCL = ganglion cell layer; DSGC – Direction-selective ganglion cell; SAC – Starburst amacrine cell; Ach – Acetylcholine; AMPA – Alpha-amino-3-hydroxy-5-Methyl-4-isoxazole Propionic Acid; NMDA – N-Methyl-D-Aspartate; BC – Bipolar cells; GABA – Gamma-Amino Butyric Acid).

1.3 Orientation Selectivity in the Retina

Orientation selectivity in the mouse retina has taken a center stage in last couple of decades as a result of observations from the OS neurons in the visual cortex. The existence of OSGCs in the mammalian retina that are tuned to either horizontal or vertically oriented stimulus has had visual neuroscientists fascinated with the way background vs an objects' edge information is processed by the retina (Levick 1967; Nath & Schwartz, 2016). Both OS amacrine cells and OS retinal ganglion cells have been identified in rabbit and mouse retina (Levick, 1967; Caldwell & Daw, 1978; Bloomfield 1991, 1994; Venkataramani & Taylor, 2010, 2016; Murphy-Baum &Taylor 2015; Nath & Schwartz, 2016, 2017). The OS tuning seen in the OS RGCs is also shown to be conserved across a wide range of sizes, velocity of stimuli and across varying degrees of background luminance (Nath & Schwartz, 2017). Furthermore, investigations conducted in the upstream pathway relaying this orientation information has brought to light the role bipolar cells and amacrine cells play in this circuitry. It has been discovered that some amacrine cells have oriented configuration that can be attributed to the elongated dendritic morphology of these cells (Bloomfield 1991, 1994).

In the vertebrate retina, wide-field amacrine cells (WACs) have been shown to be important for extraction of specific features from the visual scene, especially that of orientation-selectivity. The dendritic arbor branching and the pattern of excitatory and inhibitory inputs these neurons receive is thought to be a major reason for the OS tuning observed in the WACs in the rabbit retina (Murphy-Baum & Taylor, 2015). Such OS amacrine cells may also shape selectivity in OSGCs by providing tuned inhibition. They may also act presynaptically at the level of BC axon terminals to tune excitatory input to OSGCs (Hanson et al., 2023; Nath and Swartz 2016, 2017, Venkataramani and Taylor 2010, 2016, reviewed by Antinucci 2018). Other BC types extend their receptive fields by gap junction coupling to amacrine cells which possess oriented dendrites. There is also literature evidence for these

WACs mediating OS inhibition in certain types of retinal ganglion cells (Antinucci et al., 2016). Either these amacrine cells are selective for stimulus orientation as standalone entities or they convey OS information via inhibitory connections to retinal ganglion cells and bipolar cells or by utilizing gap junctions.

In order to better understand the circuitry involved in encoding orientation selectivity, we need to first decode where in the retina this feature first emerges. Three separate mechanisms have been proposed for this underlying OS feature in visual neurons, namely: i) Morphological properties of OS neurons, ii) Asymmetric excitation provided by the bipolar cells that make connections with the ganglion cells, iii) Inhibitory OS provided by amacrine cells mediated by transmission of GABA/Glycine onto the ganglion cells (Levick 1967; Venkataramani & Taylor, 2010, 2016; Nath & Schwartz, 2016, 2017).

For instance, in rabbit retina, it was shown that voltage clamp recordings of both excitatory and inhibitory inputs to the OS RGCs were selective for orientation. The difference noted was in the fact that the excitation was strongest in the preferred orientation, whereas the inhibitory currents measured were largest in the null orientation. Pharmacological block of GABA-A receptors in rabbit retina revealed a dramatic reduction only in the amplitude of responses observed in OSGCs while OS tuning was maintained (Venkataramani & Taylor, 2010, 2016; Nath & Schwartz, 2016).

In contrast, in the mouse retina, blocking inhibitory currents generated by the release of GABA-A or glycine independently did not affect the orientation preference observed in the OSGCs, suggesting a compensatory role for other partners (Nath & Schwartz, 2016). In contrast to the rabbit retina, complete blockage of all inhibitory conductance in the mouse retina revealed an inhibition-independent mechanism utilizing the excitatory pathway to encode orientation selectivity in the downstream output neurons. Several studies have also indicated that separate amacrine cells which have an orthogonal

orientation preference to the visual field feed inputs to BCs and possibly other OSGCs. This orthogonal preference has been attributed to the dendritic morphology of the specific OS amacrine cells in question. Depending on the dendritic stratification seen in different types of OS amacrine cells, they encode OS information either in the horizontal or vertical orientations. OS retinal ganglion cells have also been shown to be electrically coupled to OS amacrine cells via Cx36 containing gap junctions (Nath & Schwartz, 2017). Although OS amacrine cells have been identified in the mouse, rabbit, and zebrafish retina (Bloomfield 1991,1994; Murphy-Baum and Taylor 2015; Antinucci 2016; Johnston 2019) their specific connectivity patterns are only beginning to be revealed (Hanson et al., 2023).

1.4 Orientation Selectivity in ON-OFF Direction Selective Ganglion Cells

In the mammalian retina, four main types of ON-OFF DSGCs have been identified, each encoding one of the four cardinal directions (Superior, Inferior, Anterior, and Posterior) (Barlow and Hill, 1963; Barlow & Levick, 1965; Oyster and Barlow, 1967; Taylor and Vaney, 2002; Briggman et al., 2011; Taylor and Smith, 2012; Helmstaedter et al., 2013; Yonehara et al., 2013; Kim et al., 2014). To try to decode the presynaptic circuit connections, simple moving stimuli such as spots, bars, and gratings have been used to characterize the response properties of these 4 types of ON-OFF DSGCs.

A recent study carried out in posterior coding ON-OFF DSGCs in the mouse retina, has shown that these DS neurons are also selective for stimulus orientation (Hanson et al., 2023). This study showed that a specific population of bipolar cells (BC5A) are OS for vertical bars larger than their dendritic fields. Vertically oriented wide-field amacrine cell processes that contact these BC5A axon terminals were shown to be responsible for conferring this orientation selectivity to the downstream

posterior coding ON-OFF DSGCs. It was also shown that this orientation selectivity was preserved in the absence of asymmetric inhibition from SACs (Hanson et al, 2023).

Thus, OS and DS information may not be as clearly segregated into distinct pathways as originally envisioned (Barlow and Levick, 1965; Borst and Euler, 2011; Vaney et al., 2012; Levick, 1967; Caldwell & Daw, 1978; Bloomfield 1994; Venkataramani & Taylor, 2010, 2016; Murphy-Baum &Taylor 2015; Nath & Schwartz, 2016, 2017). In this thesis, I will investigate the synaptic mechanisms underlying orientation selectivity in the four types of ON-OFF DSGCs.

1.5 Direction and Orientation Selectivity in the Central Nervous System

Perception of motion of objects is vital for communication, navigation, and exteroception. Over the last several decades, motion sensing neurons have been extensively studied across different species including, but not restricted to flies, mouse, rabbits, cats, and other primates (Hubel and Wiesel, 1959; Dvork et al., 1975; Torre and Poggio, 1978; Albright et al., 1984; Reid et al., 1991; Movshon et al., 1996; Jagadeesh et al., 1997; Livingstone, 1998; Taylor and Vaney, 2002; Priebe & Ferster, 2005; Briggman et al., 2011; Joesch et al., 2013; Behnia et al., 2014; Borst et al., 2015; Ding et al., 2016; Mauss et al., 2017). DS has been documented in many places throughout the central nervous system, including but not restricted to subcortical visual pathways, and higher order cortical areas (Hubel and Wiesel, 1959; Barlow and Hill, 1963; Saul et al., 1990, 2002, 2005; Thompson et al., 1994; Xu et al., 2002). Much of the initial work was conducted in the primary visual cortex where it was observed that the response properties of a specific group of neurons were selective to the direction of motion of a stimulus (Barlow et al., 1964; Barlow and Levick, 1965).

Various models have been proposed for explaining this DS evident in the cortex (Barlow et al., 1964; Adelson & Bergen, 1985; van Santen & Sperling, 1985; De Valois et al., 2000; Peterson et al., 2004). Directional preference has been characterized by an asymmetry in the wiring between the presynaptic contacts; it has been shown that specific organization of geniculo-cortical and intra-cortical connections is needed for generating DS. Thus, cortical DS has been shown to rely on the timing of excitatory and inhibitory inputs stimulated by motion in the preferred direction (Ko et al., 2011; Cossell et al., 2015; Wilson et al., 2018; Rossi et al., 2020). Historical evidence also shows substantial differences in strength of the DS depending on the cell type and layer of interest (Cossell et al., 2015; Wertz et al., 2015; Kim & Freeman, 2016).

Another well studied circuit in the central nervous system is that of OS circuitry. This feature selectivity reflects a strong preference of neurons to edges and bars orientated along the vertical or horizontal axis in the visual field of interest. OS was first described in the primary visual cortex of cats over five decades ago (Hubel & Wiesel, 1959, 1962; Thiele et al., 2004; Monier et al., 2003; Priebe & Ferster, 2005; Zhao et al., 2013). Since then, several studies have reported that excitatory and inhibitory inputs may both be involved in establishing tuning preferences of these neurons (Thiele et al., 2004; Monier et al., 2003; Priebe & Ferster, 2005; Wilent and Contreras, 2005; Wilson et al., 2018).

Orientation preference of DS cells in the primary visual cortex has revealed that these neurons are also selective for an optimally oriented stimulus (Hubel & Wiesel, 1959, 1962; Orban et al., 1981; Emerson et al., 1992; Jagadeesh et al., 1993; Sun et al., 2016). In the visual cortex, direction and orientation information is being conveyed by ganglion cells which strongly respond to bars oriented along specific axes and moving in the preferred direction as compared to the null direction (Hubel & Wiesel, 1959, 1962, Henry et al., 1974; Weliky et al., 1996, He et al., 1998; Chen et al., 2014; Fisher et al., 2015b).

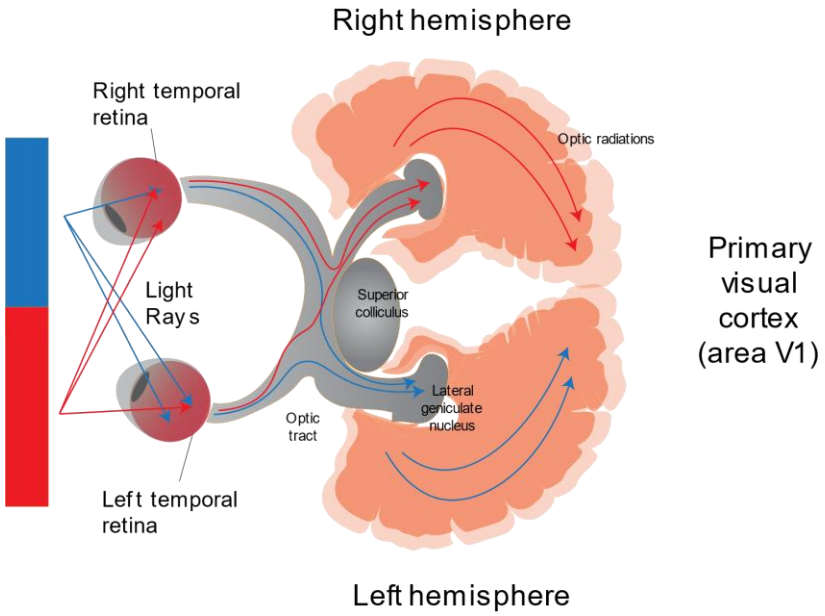

Figure 1.4 Schematic representation of the visual pathway from the retina to the primary visual cortex

Visual information from the retinal output neurons (ganglion cells) of both the eyes crosses over at the optic tract before it is sent to the lateral geniculate nucleus (LGN). The signals from the LGN are then sent to the primary visual cortex (area V1). Adapted from Scott A. Sheffield.

However, in the retina, both direction information and orientation information have been thought of as encoded by two separate population of cells. This has intrigued scientists to explore parallel processing circuits in a variety of places within the central nervous system including the retina. These findings have provided enough precedence for researchers to develop various circuit models across different species that would serve as an ideal baseline representation for a combinatorial DS and OS pathway in the mammalian retina (Hubel & Wiesel, 1959, 1962; Orban et al., 1981; Emerson et al., 1992; Jagadeesh et al., 1993; Sun et al., 2016).

1.6 Genetic Access to Single Cell Type in the DS Circuit

The emerging field of optogenetics comprises techniques that use genetically encoded light-activated proteins to manipulate cells in a minimally invasive way using light. An optogene confers light sensitivity to any targeted neuron and thereby functionally turns it into artificial photoreceptors (Fenno et al., 2011). The most prominent example is channelrhodopsin-2 (ChR2), which allows the activation of electrically excitable cells via light-dependent depolarization (Nagel et al., 2003).

In the mouse retina, channelrhodopsin-2 (ChR2), has created opportunities for circuit-specific modulations to stimulate specific cell types. Optogenetic manipulations to isolate specific components of the DS circuitry have shown that direct activation of ChR2 expressed in starburst amacrine cells produces robust direction selectivity under photoreceptor/bipolar cell blockade (Sethuramanjuam et al., 2016; Hanson et al., 2019). Other studies have shown ON bipolar cells that were engineered to be photosensitive (Lagali et al., 2008), also specifically in BC5As which provide input to posterior coding ON-OFF DSGCs (Hanson et al., 2023).

Although there exists a significant difference of several orders of magnitude in the number of photons required to activate ChR2 ($\sim 10^{15}$ photons cm^{-2} s^{-1}) when compared to the intensity of light that is required to stimulate endogenous photopigments ($\sim 10^{10}$ photons cm^{-2} s^{-1}), many of the response properties of the cells that express the photosensitive ChR2 have been shown to be conserved across time points (Bi, A. et al., 2006; Lagali et al., 2008; Sethuramanujam et al., 2016; Hanson et al., 2019, 2023). The time course of the response recorded from ChR2 mediated experiments has shown to be faster than the traditional processing time of information conveyed in wild type animals because of the signal from bipolar cells bypassing a synapse.

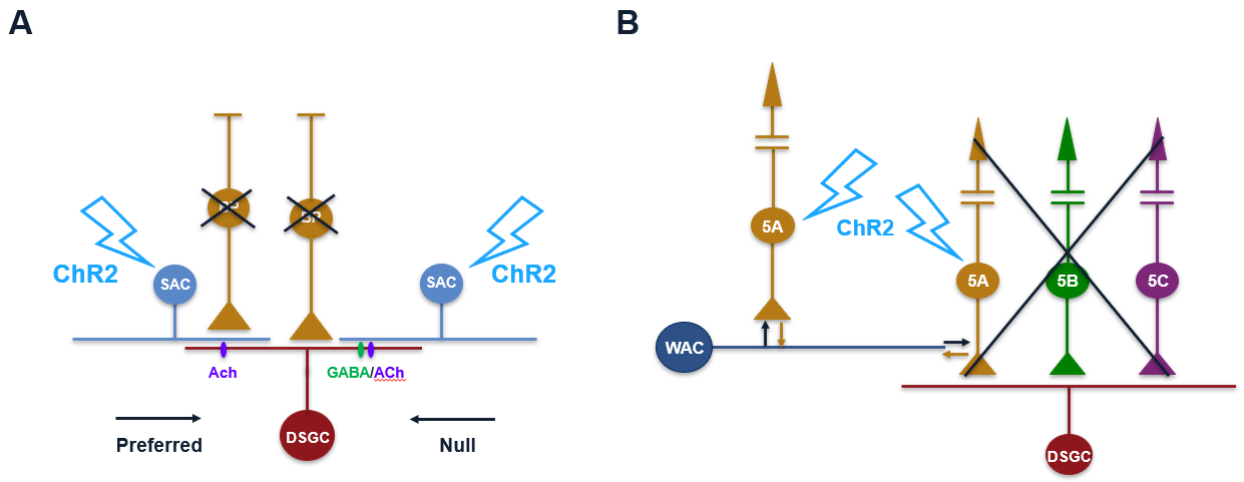

Figure 1.5 ChR2 experimental design

(A) Schematic of the DS circuitry where ChR2-expressing SACs (ChAT-cre-ChR2) will be specifically targeted for performing experiments after blocking off photoreceptors to bipolar cell synaptic transmission and artificially stimulating the SACs with bright light (~10^{15} photons cm^{-2} s^{-1}). **(B)** Schematic representation of wide-field amacrine cell and bipolar cell network where ChR2-expressing BC5As (Kcng4cre-ChR2+) will be specifically targeted for performing experiments after blocking off photoreceptors to bipolar cell synaptic transmission and artificially stimulating the BC5As in the periphery (long bars with central occlusions) with bright light (~10^{15} photons cm^{-2} s^{-1}). (DSGC – Direction-selective ganglion cell; SAC – Starburst amacrine cell; Ach – Acetylcholine; AMPA – Alpha-amino-3-hydroxy-5-Methyl-4-isoxazole Propionic Acid; NMDA – N-Methyl-D-Aspartate; BC – Bipolar cells; GABA – Gamma-Amino Butyric Acid).

For this thesis, I will outline the experimental design used to target ChR2 expressing SACs (Figure 1.6A) and BCs (Figure 1.6B) for direct stimulation after blocking off photoreceptor to bipolar cell signal transmission using pharmacology. Whole cell patch-clamp recordings from ganglion cells can be used to gain insights into the synaptic processing underlying the formation of spiking responses, IPSCs and EPSCs through ChR2 activation of the bipolar cells (Lagali et al., 2008; Hanson et al., 2023) or starburst amacrine cells (Sethuramanujam et al., 2016; Hanson et al., 2019) after blocking off - photoreceptive to bipolar cell transmission of light information.

1.7 Objectives

Processing of visual information is known to begin in the complex circuits of the retina. Here, multiple overlapping microcircuits serve to extract distinct features of the visual world. A major challenge is to identify the cellular components of each of these circuit and understand their functional properties. To this end, the DS circuit has served as a model system. Interestingly, recent work has shown that one of these bipolar cell types, the BC5A, is tuned for orientation abut not direction. However, whether the other BCs driving the circuit are also similarly tuned for orientation is not clear. And importantly, whether all the 4 types of ON-OFF DSGCs receiving input from overlapping sets of BCs can encode stimulus orientation remains to be tested. The objective of this research is to dissect the circuit elements involved in encoding orientation selectivity in the retina as an additional visual motif by means of harnessing the DS circuitry.

In this thesis, I will describe the neural basis for two types of stimulus specificity – namely direction coding and orientation coding. I will characterize the tuning properties of ON-OFF DSGCs using electrophysiology, two-photon imaging, pharmacology and optogenetics. I will focus on all four types of ON-OFF DSGCs, and how both direction and orientation information is computed concurrently. I will also outline the mechanisms involved in imparting this directionality and OS tuning by selectively manipulating different components of the circuitry in order to characterize where in this DS circuitry, OS information first emerges.

2. Methods

2.1 Animal Care

The majority of the recordings from ON-OFF DSGCs were obtained from retina harvested from non-transgenic C57BL/6J (RRID: IMSR_JAX:000664) mice. The DSGCs were identified by their directional tuning properties. However, a few experiments were performed using retinal tissue isolated from transgenic mouse models namely the Trhr+::eGFP (provided by Dr. Marla Feller, UC Berkeley; RRID: MMRRC_030036-UCD) mouse line in which posterior coding DSGCs are labelled, and from Hb9::eGFP mouse line in which ventral coding DSGCs are selectively labelled (Trenholm et al., 2011). To investigate the role of electrical coupling, the Kcng4-cre (B6.129(SJL)-Kcng4$^{tm1.1(cre)Jrs/J}$, JAX stock #029414) was crossed with Cx36-floxed line (provided by Dr. David Paul, Harvard). Both single floxed and double floxed Cx36 transgenic mice were used for experiments as control and complete knockout models. The Channelrhodopsin (ChR2) experiments were carried out in retina harvested from Kcng4cre-ChR2+ mouse line where the cre line labels type 5a (BC5A) ON bipolar cells and a ChAT-Cre-ChR2 mouse line (RRID: MGI_5475195) crossed with Ai32 (RRID: MGI_5013789), to selectively express ChR2 in SACs. Photosensitivity of ChR2-expressing bipolar cells and post-synaptic visual signal transduction was tested electrophysiologically by whole-cell patch clamp recordings of retinal ganglion cells in electroporated retinas. Mice of both sexes were used for experiments between P21-P140 ages. Mice were housed and maintained on a 12-hour light/dark cycle. All procedures were carried out in accordance with the Canadian Council of Animal Care (CCAC) and approved by the University of Victoria's Animal Care Committee.

2.2 Retinal Preparation

Mice brought to the lab from the animal care facility were dark adapted for approximately 45 minutes to an hour before carrying out the experiments. The animals were anesthetized with 5% isoflurane and euthanized by cervical dislocation before the eyes were removed. Retina dissections were performed under a night vision microscope (equipped to detect IR light). During the dissection, a small incision was made to identify the orientation of the retina. Isolated retinae were laid photoreceptor side down on a 0.45 µm membrane nitrocellulose filter (Millipore, Bedford, MA, USA) with a pre-cut window, through which images were focused onto the retina. Visualization under IR illumination utilized a Spot RT3 charge coupled device camera (Diagnostic Instruments, Inc., Sterling Heights, MI, USA) attached to an upright Olympus BX51 WI fluorescent microscope, equipped with a 60x water immersion lens (Olympus Canada Inc., Markham, Ontario, Canada).

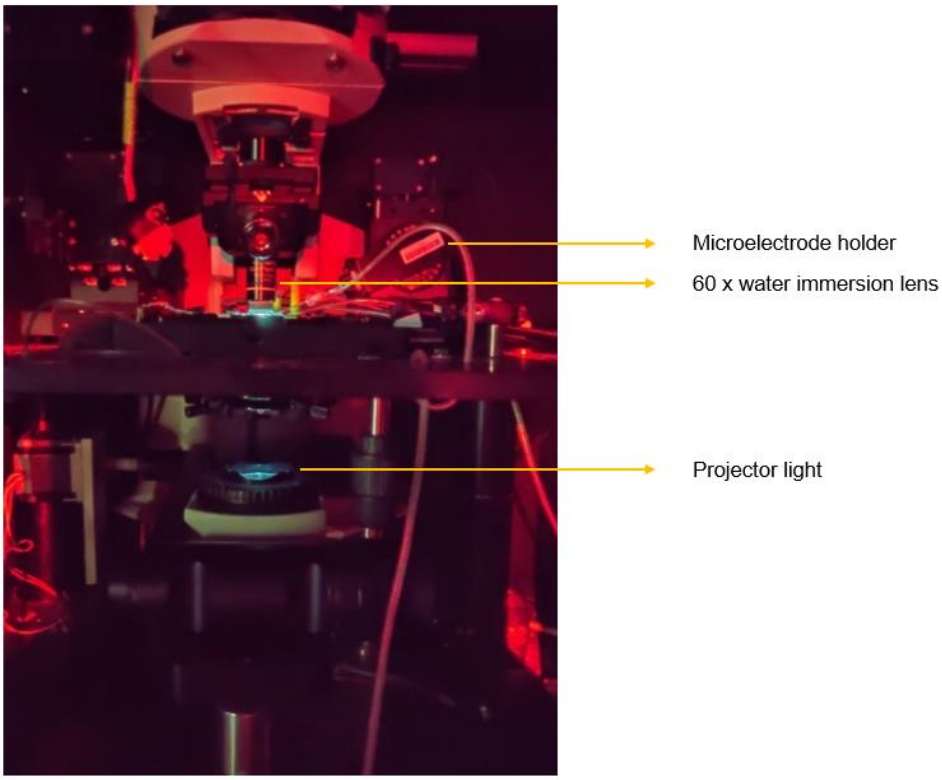

Figure 2.1 Electrophysiology experimental setup

Olympus BX51 WI fluorescent microscope, equipped with a 60x water immersion lens. Microelectrode holder containing a glass electrode to measure electrical activity from retinal neurons. Light from the projector is flashed from below the setup.

After removal of vitreous humor the dissected retinae were continuously bathed with Ringer' solution containing (in mM): 110 NaCl, 2.5 KCl, 1 CaCl2, 1.6 MgCl2, 10 dextrose, and 22 NaHCO3 on a chamber containing a hydrophilic, non-sterile filter paper and continuously perfused with carbogen (95%O2:5% CO2) and ringer's solution containing 110 mM NaCl, 2.5 mM KCl, 1 m CaCl2, 1.6 mM MgCl2, 10 mM dextrose and 22 mM NaHCO3, maintained at 35-37°C. Perfusion rates were maintained at ~3 ml/min. For each experiment, the ventral axis of the retina was identified based on the scleral landmarks (Wei et al., 2010) was marked with a small cut and mounted on the filter paper. In the experiments performed across different days, the retina was also mounted in various orientations to ensure that the orientation-selectivity observed was not due to a bias in the experimental setup.

Responses were normalized to the dorsal/ventral axis of the retina. Inhibitory/excitatory blockers and other drugs added to 25ml of Ringer's solution. The drug infused solution was washed into the perfusion system and directed towards the chamber containing the retinal tissue with continuous flow of drug infused Ringer solution. For the ChR2 experiments, 20 μM L-AP4 (Abcam Biochemicals) and 10 μM UBP-310 (Abcam Biochemicals) were perfused to block the ON and OFF photoreceptor responses, respectively. To isolate AMPA and NMDA mediated events, either 50 μM D-AP5 (Alomone Labs) or 10 μM NBQX disodium salt (Alomone Labs) were washed on and circulated through perfusion. CNQX and DCG-IV were purchased from Tocris, D-AP5 was purchased from Alomone and UBP-310 was purchased from Abcam. Unless otherwise noted, all other reagents were purchased from Sigma-Aldrich Canada.

Only cells with a direction selectivity index (DSI; calculated based on the normalized vector sum of responses in eight directions) greater than 0.3 were considered for this analysis.

2.3 Whole-Cell Patch-Clamp Recordings

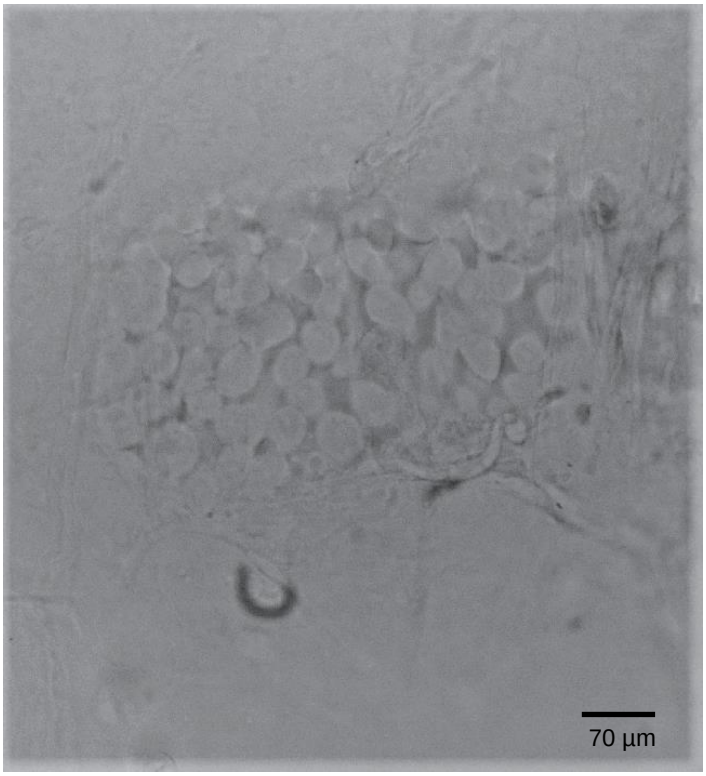

Figure 2.2 Wholemount retina with ganglion cell layer side up

Ganglion cell layer of the mouse retina after the inner limiting membrane was removed to measure electrical activity from ON-OFF DSGCs after characterizing their extracellular spiking responses.

Extracellular spike recordings were made using a loose seal (25–50 MΩ) with 6–10 MΩ electrodes filled with Ringer solution. Cells identified based on the extracellular spike recordings were then patched for whole cell recordings using a 5–7 MΩ electrode. For voltage clamp recordings,

electrodes contained (in mM): 112.5 CsCH3SO3, 9.7 KCl, 1 MgCl2, 1.5 EGTA, 10 HEPES, 4 ATP Mg2, and 0.5 GTP Na3. The pH was adjusted to 7.4 with CsOH. Intracellular voltage clamp and current clamp recordings were made using ~3-6 MΩ electrodes. DSGCs were identified by their genetic labeling or by their characteristic DS responses.

To isolate excitatory and inhibitory synaptic inputs, each cell was held at the reversal potential for inhibition (~ 60 mV, i.e., reversal potential for chloride (ECl)) and excitation (~ 0 mV), respectively. Recordings were made with a Multiclamp 700B amplifier (Molecular Devices Inc, Sunnyvale, CA). Signals were digitized at 10 kHz (PCI-6036E acquisition board, National 9 Instruments) and acquired using custom software written in LabVIEW ™. Clampex 10.1 software (Molecular Devices) was used to control the voltage command outputs, acquire data and trigger stimuli. SAC activity was blocked with bath application of DCG-IV ((2S,2′R,3′R)-2-(2′,3′-dicarboxycyclopropyl) glycine) for measuring the OS tuning of ON-OFF DSGCs. Excitatory OS responses were partially blocked using a low concentration (4 µM) of AMPA/kainite receptor antagonist 6-cyano-7- nitroquinoxaline-2,3-dione (CNQX).

2.4 Receptive Field Centering

Different ON-OFF DSGCs have morphologically distinct dendritic fields that have varying shapes. The excitatory and inhibitory inputs onto these ON-OFF DSGCs provide either an asymmetric or symmetric receptive field, which varies according to the cell type (Awatramani & Slaughter, 2000; Borges & Wilson, 1987; Dacey et al., 2000; Devries, 2000; Hare & Owen, 1990; Ichinose et al., 2014; Kaneko, 1973; Werblin & Dowling, 1969). These inhibitory and excitatory regions together form a single receptive field selective for stimulus shape fitting for each ON-OFF DSGC in question. The

extent of the dendritic span across which a spiking response can be measured at the soma is critical to determine the shape or structure of the receptive field (Yang and Masland, 1992, 1994).

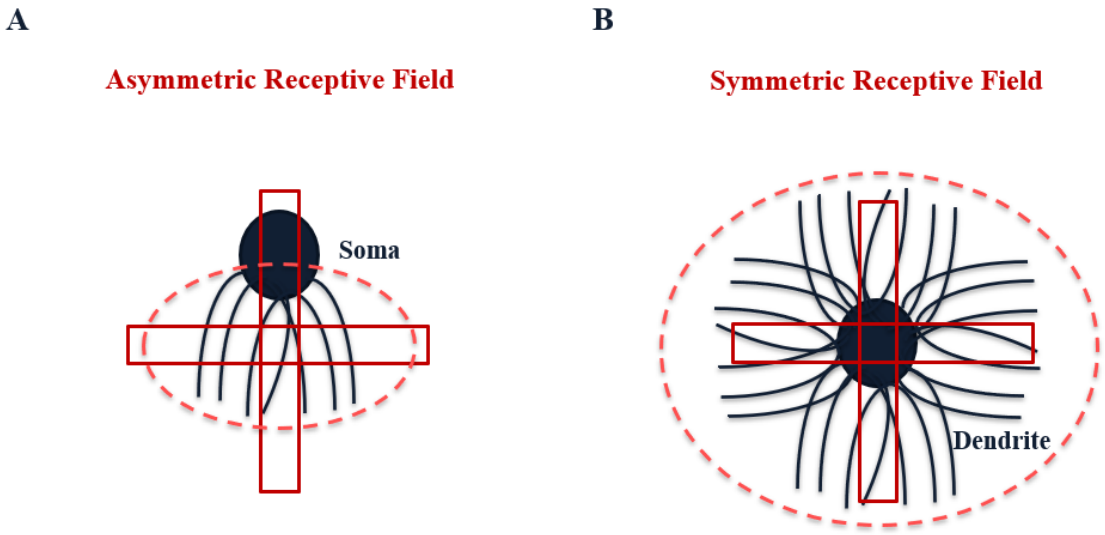

Figure 2.3 Receptive field types

(A) Example of an asymmetric (dendritic segments are unequally distributed on all sides) receptive field of an ON-OFF DSGC. **(B)** Example of a symmetric (dendritic segments are equally distributed on all sides) receptive field of an ON-OFF DSGC.

Responses to stationary bars (100 x 600 µm) flashing 200 µm away from the soma of the ON-OFF DSGCs and moving from one side along the horizontal or vertical axes, flashing every 50 µm while traversing the length of the dendrite to the soma were measured. Responses to sstationary bars (100 x 600 µm) flashing at intervals of 50 µm away from the soma, moving until about 200 µm away from the soma were measured. Averaged peak spike rates from the horizontal and vertical fields were plotted against the distance from the soma as a line graph to realize the shape of the receptive field. These values were then used to identify the center of the receptive field and the stimulus center was aligned to the receptive field center of the ON-OFF DSGCs. Once the stimulus was centered, the spiking

responses of these ON-OFF DSGCs to static bars (100 x 600 µm) flashing in 8 different orientations were measured.

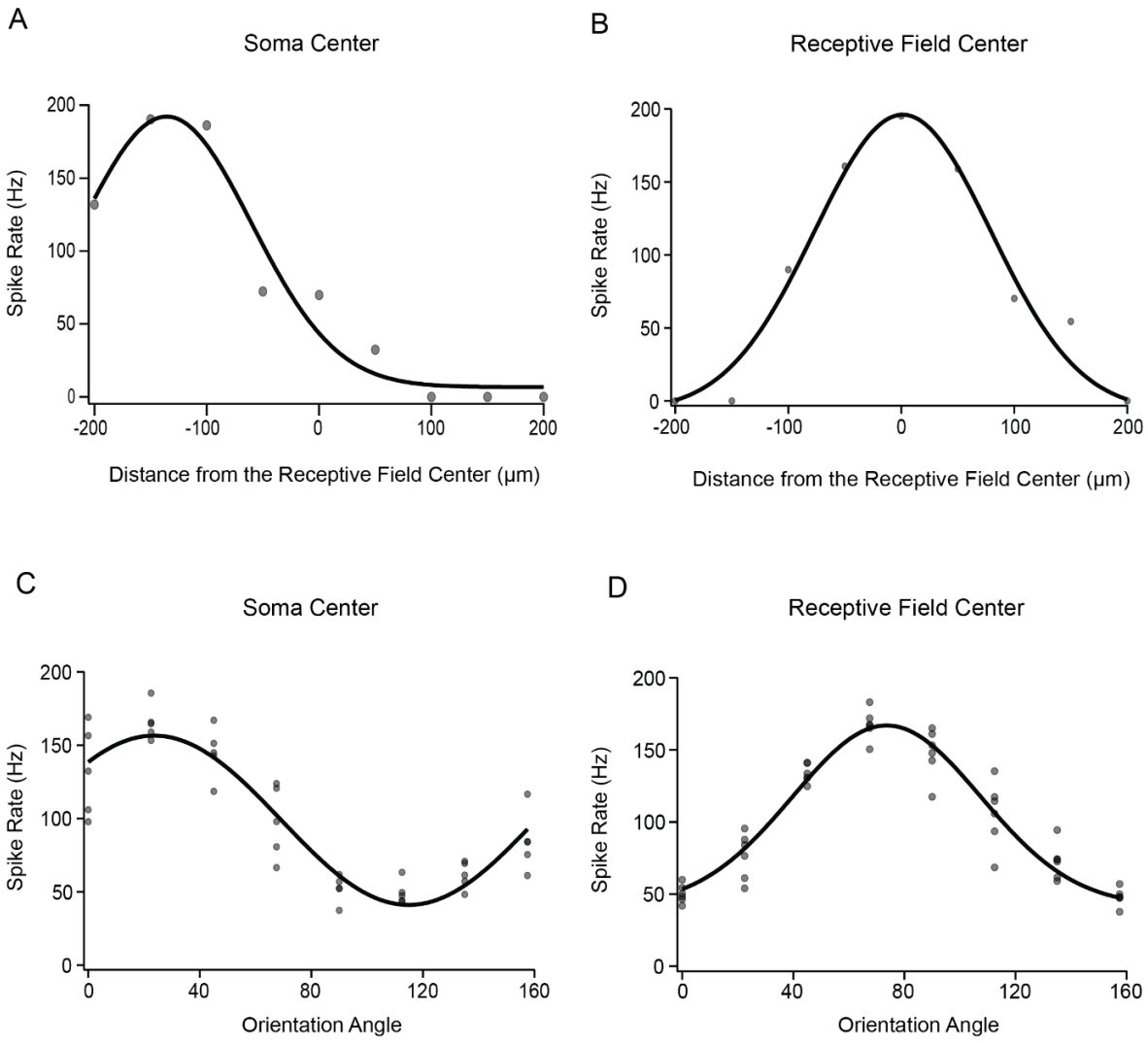

Figure 2.4 Receptive field centering

(A) Peak spike rates obtained from a dorsal coding DSGC flashing a (100 x 600 µm) bar along the length of the dendritic field to map out the receptive field of the ON-OFF DSGC. **(B)** Peak spike rates obtained from a dorsal coding DSGC flashing a (100 x 600 µm) bar along the length of the dendritic after aligning the stimulus to the center of the ON-OFF DSGC's receptive field from an example dorsal

coding cell. **(C)** Average OS tuning curve constructed from peak spike rates obtained from a dorsal coding DSGC with stimulus centered on the soma. The individual grey dots represent separate trials. **(D)** Average OS tuning curve constructed from peak spike rates obtained from a dorsal coding DSGC with stimulus centered on the receptive field center. The individual grey dots represent separate trials.

2.5 Light Stimulation

Stimuli (spots, bars, and masked gratings) were generated with a digital mirror light projector (Texas Instruments; refresh rate 75 HZ) controlled with custom software written by Dr. David Balya (Friedrich Meischer Institute, Switzerland) based on the Psychophysics toolbox extension for Matlab (Brainard, 1997). Custom software (Stimgen) was used along with protocols written in Matlab for creating stimulus packages. The ambient background intensity, measured with a calibrated spectrophotometer (USB2000, Ocean Optics), was reported as rhodopsin photoisomerizations per second (R*/s; derived from the absorption spectrum of mouse photoreceptors; Lyubarsky et al., 1999). Most of the experiments utilized intensities that were expected to favor rod responses (less than 13 R*/s; Farrow et al., 2013; Grimes et al., 2014b) and sometimes bright light stimulus were used to enable cone-dominated responses. Neutral density filters were used to control the stimulus light intensity.

Light stimuli, projected from below the preparation, were focused with a substage condenser onto the photoreceptors, centered over the soma and the measured receptive field of the recorded neuron. The visual stimuli were created using positive contrast settings ranging between 20% and 1000%. For determining directionality of the DSGCs, light evoked activity was measured for two different bar stimuli, namely, 600 x 100 µm (long bar) and 100 x 600 µm (wide bar) moving across the visual field in 8 different directions (0°, 45°, 90°, 135°, 180°, 225°, 270°, 315°). For measuring the orientation selectivity of the identified DSGCs, light evoked activity was measured for 100 x 600 µm bars flashing from a stationary point in the field in 8 different orientations (0°, 22.5°, 45°, 67.5°, 90°,

112.5°, 135°, 157.5°). Detailed orientation tuning curves were made by presenting static bars at specific angles with pre-determined orientation at the center of the receptive field (RF). ChR2 (Channelrhodopsin 2) activation was achieved through stimulation using an intense bright light (ʎ = 400-700nm) as shown previously (Sethuramanujam et al. 2016).

2.6 Analysis of Physiological Data

Physiological data was analyzed using custom routines written in Matlab (Mathworks) or Igor (Wavemetrics). Spike numbers or peak spike rates were reported for extracellular or current clamp recording analysis. Spike rate was estimated by filtering the light evoked spike train using a convolution with a Gaussian kernel with a fixed width, σ = 25 ms. Responses were averaged over multiple trials (2-5). Either peak amplitude or integrated postsynaptic currents were used to quantify light-evoked synaptic current responses, but no qualitative differences were observed between these two methods. Population data have been expressed as mean ± SEM and are indicated in the figure legend along with the number of samples. Student's T-test was used to compare values under different conditions, and the differences were considered significant when $p \leq 0.05$. Statistical power is reported as the result of the said student's t-test, with significance levels as reported.

A direction selectivity index (DSI) and orientation selectivity index (OSI) were quantified as the vector sum of the responses measured in all 8 directions calculated as shown in the equation:

$$DSI = \frac{\sum R(\theta)e^{i\theta}}{\sum R(\theta)} \quad OSI = \frac{\sum R(\theta)e^{2i\theta}}{\sum R(\theta)}$$

where R(θ) is the response for θ direction or orientation calculated from the spike rate or peak

EPSC/IPSC amplitude during that stimulus. PD and ND are responses recorded to stimulus moving in the preferred and null direction, respectively. These indices range from 0 to 1, where 1 represents strongest suppression and 0 represents equal responses to preferred and non-preferred stimuli. Direction and orientation tuning widths were estimated using a Gaussian function (Nowak et al., 2011).

3. Results

3.1 Four types of ON-OFF DSGCs encoding the cardinal directions exhibit an orientation selectivity that is orthogonal to their preferred-null axes

In a recent Ca^{2+} imaging study, it was demonstrated that type 5A bipolar cell (BC5A) axon terminals, which are known to be anatomically connected to DSGCs and starbursts, exhibit a strong bias for vertically oriented stimuli (Hanson et al., 2023). Such selectivity appears to be mediated by a specific type of wide-field amacrine cell (WF5A), originally not thought to be making excitatory connections, but which we now is inferred to make mixed glutamatergic/electrical connections with BC5A input through their vertically oriented processes (Figure 3.1, left; Hanson et al., 2023).

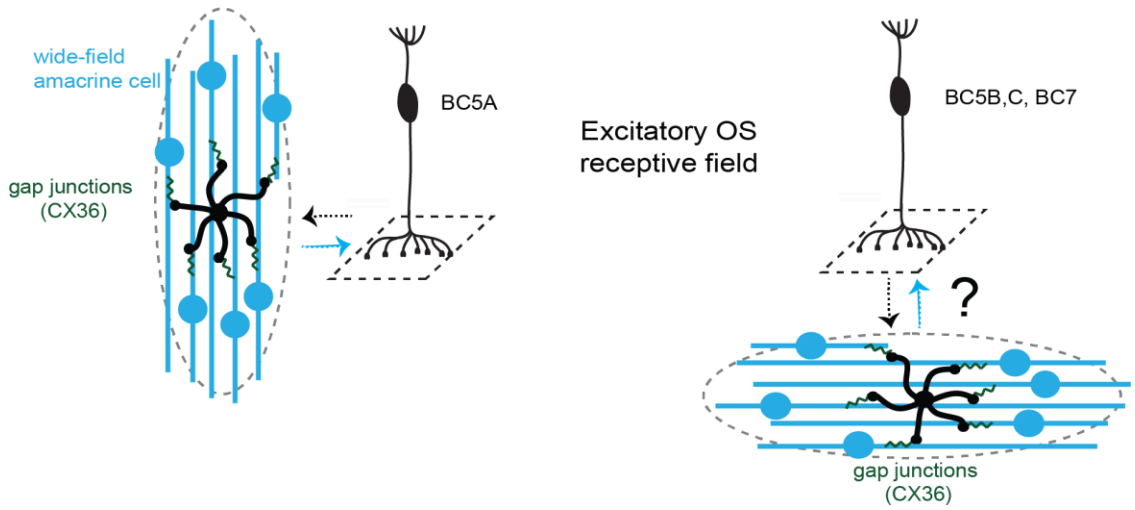

Figure 3.1 Wide-field amacrine cell and bipolar cell electrical network

Excitatory OS mechanisms involving electrical connections between BC5A (left, Hanson et al., 2023) or possibly other BCs (right, hypothesis) and wide-field amacrine cells, possibly conferring OS in downstream ON-OFF DSGCs. The black and blue arrows represent reciprocal gap junction coupling between BCs and WACs. Adapted from Hanson et al., 2023.

Tuned bipolar cells appear to drive a vertical orientation selectivity in nasal-coding DSGCs labelled in the TRHR-GFP transgenic mouse line, independent of the asymmetric starburst circuitry (Figure 1.3B; Hanson et al., 2023). However, the extent to which other types of BCs and DSGCs in the circuit are tuned for orientation remains to be fully investigated.

To determine if orientation-selectivity is a general property of all four types of DSGCs, I characterized their spiking properties in a whole-mount retinal preparation (Figure 3.2A, B). DSGCs were identified based on the directional tuning properties of their ON and OFF spiking responses evoked by moving bars (8 directions, 1000 um/s). In these experiments, the dorsal pole of the retina was notched before being placed in the recording chamber (Figure 3.2A), which allowed to estimate the DSGC's directional preference relative to the retinal axes. As expected, I found that the preferred directions of individual DSGCs clustered around the cardinal directions (Figure 3.2C). Although there was overlap between clusters (as preferred directions vary with retinal location; Sabah et al., 2021), for simplicity, I assigned DSGCs to dorsal-, ventral-, nasal-, or temporal-coding types based on the cardinal direction which was closest to their preferred direction (i.e., within + 45 degrees of a given cardinal direction). I found the preferred directions of all genetically labelled TRHR+ DSGCs to fall within 39±5 degrees of the nasal direction, consistent with a previous study (Rivlin-Etzion et al., 2011). The location of all the individual cells relative to the optic disc of the retina has been plotted (Figure 3.3).

When I probed their receptive field properties with static oriented bars (100 x 600 um bars; flashed for 2 seconds in 8 orientations in equal increments of 22.5◦ spanning 0 to 180 degrees), I observed orientation selectivity in all four types of DSGCs (Figure 3.2D-F). On average, the spiking response to a bar of a preferred orientation was roughly twice as strong as that evoked by a bar that was orthogonal to it ('null' bar). In these experiments, I took care to center the stimulus over the DSGC's receptive field (Figure 2.4.2), to ensure that the observed selectivity for orientation did not arise simply

from displaced stimuli. Orientation selectivity was quantified using an orientation selectivity index (OSI, calculated as the vector sum of responses measured across 8 stimulus orientations). The OSI distributions of all four types of DSGCs were similar to each other (Figure 3.2D), although ventral coding DSGCs had marginally higher OSI values. These OSI distributions are also similar to those measured in OSGCs (Nath & Schwartz, 2017) and the OS observed was stable over a range of stimulus contrasts (Figure 3.2E). However, it must be noted that the peak spike rate and number evoked by moving bars were considerably larger for moving vs static bars.

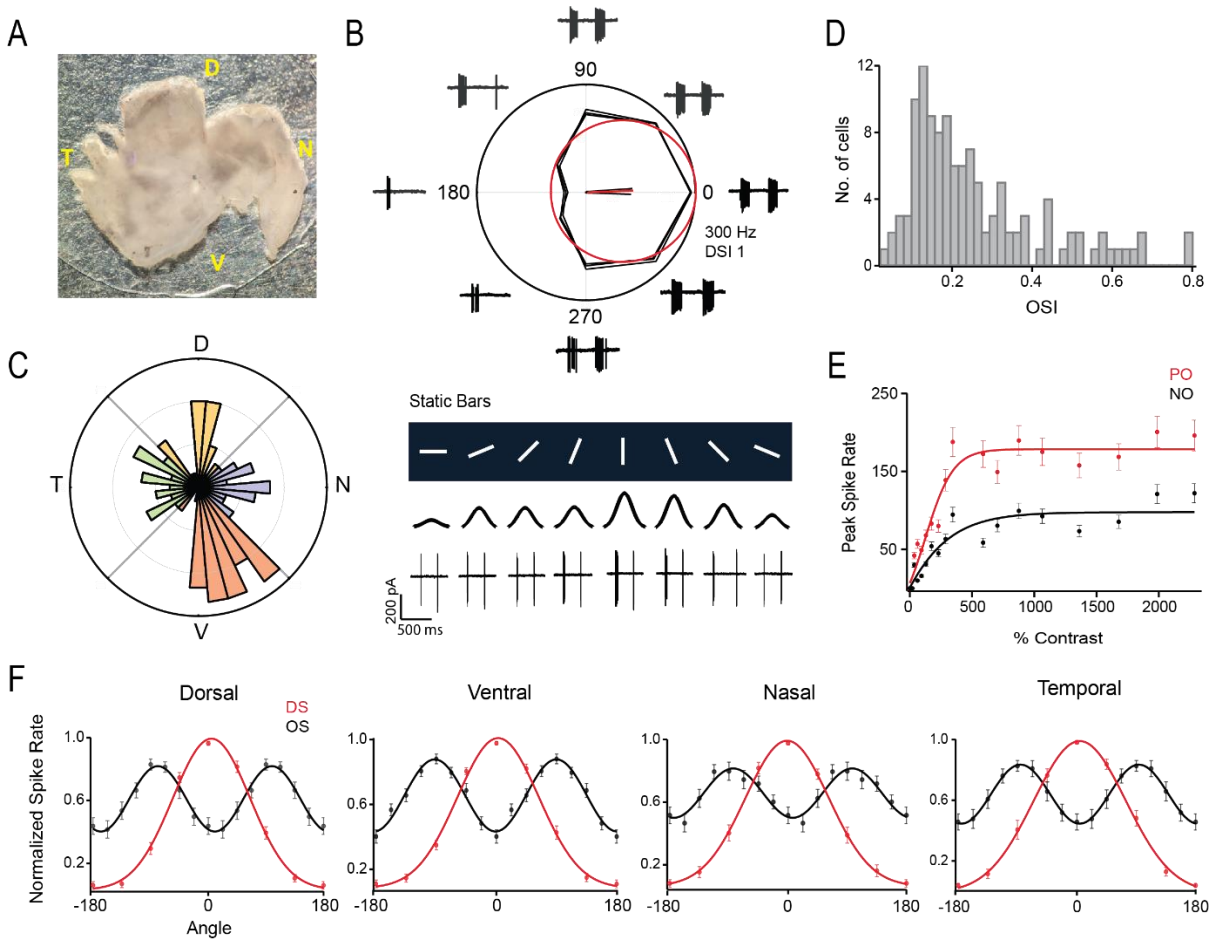

Figure 3.2 Orientation selectivity in all 4 types ON-OFF DSGCs

(A) Retinal preparation marked with a small cut along the ventral axis and mounted on a glass slip coated with polylysine. **(B)** DS tuning from an example dorsal coding DSGC represented as a polar graph calculated from the peak spike rate during 8 direction stimulation (0 to 360◦ in increments of 45◦) with spiking responses normalized to the DS peak angle to be along 0° shown across the polar graph (top) (Black = individual trials, Red = average). OS tuning obtained from the same dorsal coding DSGC showing peak spike threshold and spiking responses shown for all 8 stimulus angles (bottom). **(C)** Vector sum of all 4 types of ON-OFF DSGCs represented in a polar histogram split across 4 cardinal axes (n=117 cells). All cardinal axes are color coded differently. The magnitude shows the number of cells within a given wedge range. The angles show the absolute vector sum angle of all the cells. **(D)** Histogram of OSI across the population calculated as the vector sum of responses from static bars flashing in 8 orientations (n=117 cells). **(E)** Contrast response function curve showing peak spike rates for preferred orientation (PO) and null orientation (NO) represented as a function of % contrast (n=10 cells). Data shown as mean ±SEM. **(F)** Relationship between preferred direction (Red) and preferred orientation (Black) across the 4 different populations of DSGCs (n=117 cells), OS and DS responses are normalized together to the peak spike rate of DS averaged over a few trials for each cell and fitted with a gaussian function. Data shown as mean ±SEM.

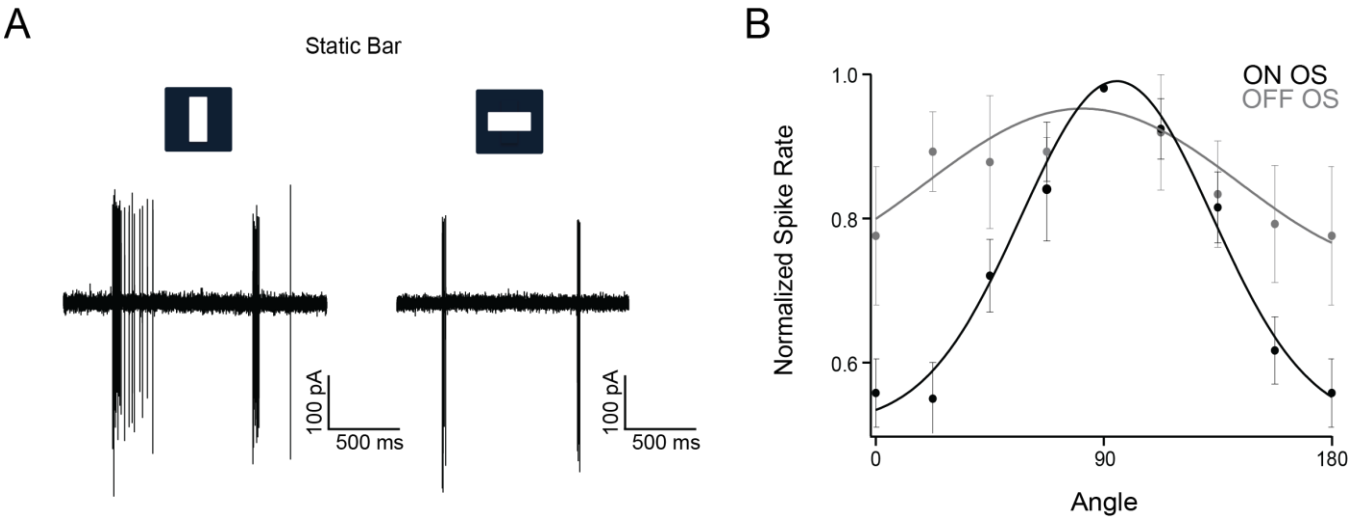

Figure 3.3 OFF OS in all 4 types ON-OFF DSGCs

(A) Sample post-synaptic spiking traces obtained from ON-OFF DSGCs for preferred and null orientations of a static bar stimulus. **(B)** Normalized OS tuning curves for both ON and the OFF responses. Spike rates obtained for the OFF responses were lower than that of ON responses (n = 117 for ON, n = 34 for OFF). The responses are normalized to the peak spike rate for both ON and OFF responses. Also see Figure 3.7 for ON and OFF EPSC.

Strikingly, in every instance, the preferred orientation was orthogonal to the DSGC's preferred-null (PN) axis defined by moving stimuli. This can be seen when the DS and OS tuning curves are plotted together. In all cases the peaks of the OS and DS tuning curves estimated using a Gaussian function were offset by 90°. Note, since the stimulus direction spans a greater range (0° to 360°) compared to stimulus orientation (0° to 180°); the OS tuning curve was duplicated to fill the axis range. While the direction tuning was significantly sharper, in that the null motion responses were significantly weaker than the null bar responses, the tuning width was sharper for orientation compared to direction (average FWHM). Together, these results suggest robust OS mechanisms shape the responses of all type of DSGCs. In the next sections I will examine the properties of excitatory and inhibitory network mechanisms and test how they contribute to OS.

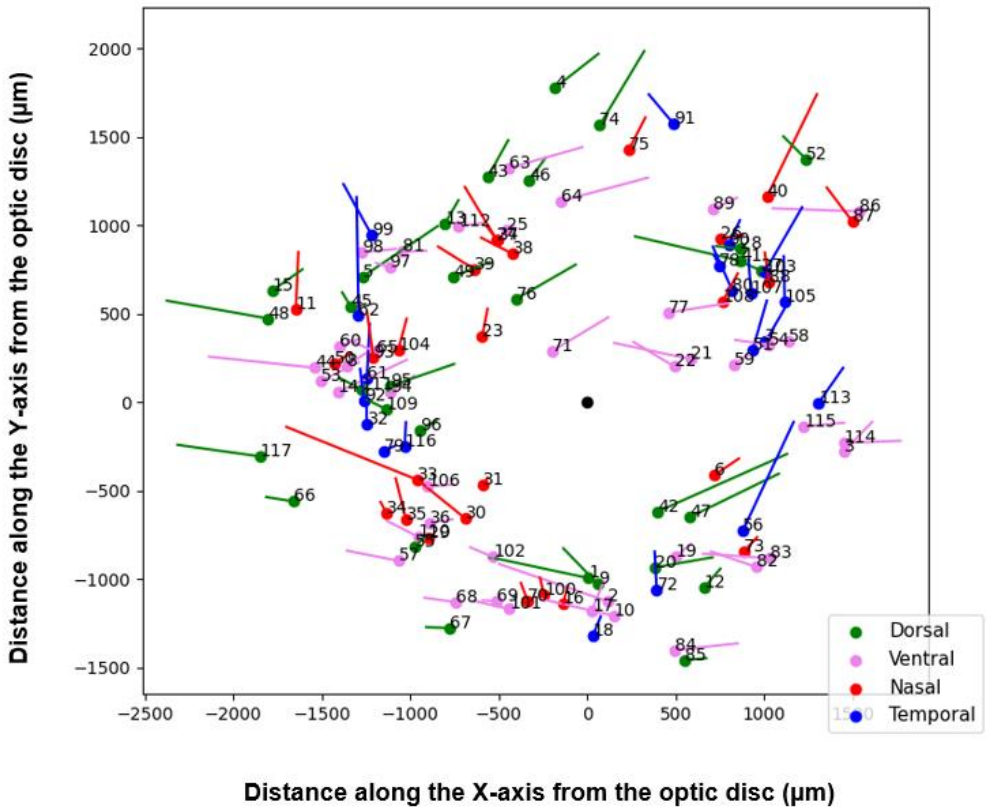

Figure 3.4 – Individual cell locations in the retina

X and Y coordinates of all the individual cells' locations obtained from various retinas across different days (n=117 cells). Location of each cell recorded is the location of each circle. The color of the circle indicates the DS coding (Dorsal, ventral, nasal or temporal. The length of the vectors (line) represents the strength of the orientation selectivity index. The direction of the vectors represents the vector sum angle of orientation for a static bar.

3.2 All four ON-OFF DSGC types receive vertically tuned glutamatergic excitation mediated by electrically coupled BC5As

Multiple types of bipolar cells make synaptic connections with ON-OFF DSGCs, namely, ON BCs type 5A, type 5B, type 5C, and type 7, and OFF BCs type 3A, type 3B and type 4 (Helmstaedter et al., 2013; Greene et al., 2016). Anatomical studies suggest that BC5As provide common input to all four types of DSGCs, which is puzzling in view of our result showing that D/V coding DSGCs have an orientation selectivity along the horizontal axis (orthogonal to their PN axis). However, previous connectomic analysis did not examine the connectivity to each different type of DSGC in isolation. Hence, it is conceivable that D/V coding DSGCs receive a greater proportion of their glutamate input from the other BCs in the DS circuit (ON BC5A, 5B, 5C, and/or BC7, and OFF BC3A, 3B and/or 4; Helmstaedter et al., 2013; Greene et al., 2016; Ding et al., Kim et al., 2014), that are tuned along the horizontal axis, in line with their orientation selectivity.

To test this possibility, I next monitored BC output as glutamatergic EPSCs in voltage-clamped DSGCs. To isolate responses mediated by AMPA and NMDA receptors, these measurements were made at a holding potential of -30mV (to remove the Mg2+ ion blocking NMDA receptors) in the added presence of $GABA_{A\&C}$ and nicotinic ACh receptor antagonists (5 µM SR95531, 50 µM TPMPA, 5 µM Hexamethonium).

Consistent with our previous study, in which I found that BC5A OS tuning persists when chemical synaptic transmission in the inner retina is blocked, responses evoked by flashing bars were strongly OS. Interestingly, excitatory inputs to NT and DV coding cells were both tuned for vertical orientations. Similar tuning patterns could also be observed when a 400 µm mask was centered over the DSGC's receptive field (~200 µm in diameter) consistent with the idea that they are mediated by the extensive vertically oriented processes of wide-field amacrine cells. These masks were used in the middle of the bar to occlude the center and stimulate the surround, thereby targeting the BC5A which are thought to be present at the farthest end, making synaptic contacts with WACs as shown in the (Figure 3.5). The similarity in the input properties indicated that all types of DSGCs receive information from a common set of BCs. They also demonstrate that DV coding cells do not receive horizontally tuned input. In fact, DV coding DSGCs receive a maximal glutamate input when bars are presented in their null orientation (Figure 3.6A, B).

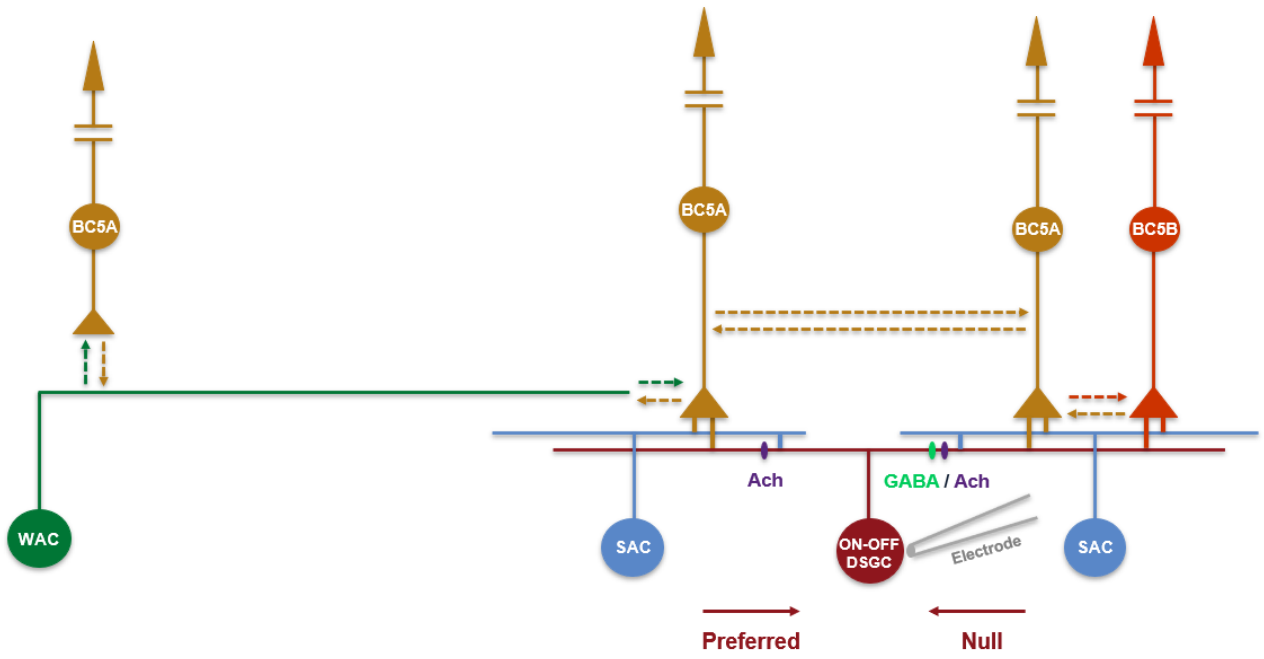

Figure 3.5 Schematic representation of wide-field amacrine cell and bipolar cell network

Reciprocal electrical connectivity between BC5A and WAC (represented with green and yellow arrows), involving lateral WAC connections to central DS network. WAC – Wide-field amacrine cell; DSGC – Direction-selective ganglion cell. BC5A, BC5B, BC5C – Bipolar cell types 5A, 5B, SAC – Starburst amacrine cells. Ach – Acetylcholine; AMPA – Alpha-amino-3-hydroxy-5-Methyl-4-isoxazole Propionic Acid; NMDA – N-Methyl-D-Aspartate; GABA – Gamma-Amino Butyric Acid. Adapted from (Hanson et al., 2023).

Next, to investigate whether the tuned input arises mainly from BC5As or whether other BCs in the circuit are also tuned for orientation, I measured responses in a mouse line in which Cx36 gap junctions were selectively removed from BC5As (KCNG4-Cre:: $Gjd2^{fl/fl}$; Hanson et al., 2023). Connexin36 (Cx36) has been previously shown to be the major gap junction protein expressed by BC5A (Shekhar et al., 2016). In this mouse line, direction selectivity is preserved (Figure 3.8) but the peak amplitude of the EPSCs measured in DSGCs were significantly diminished and were not tuned for orientation. While stimulating the center failed to produce OS tuning in these ganglion cells, activating the surround by introducing a mask to occlude the center receptive field did not generate any response in these cells. In other words, the vertically tuned surround excitation previously observed in wild type mice models were abolished in the Cx36 KO retinas (Figure 3.6C, D). This failure to evoke EPSCs from the lateral connections confirms that knocking out connexin 36 containing gap junction between BC5A and WACs abolished the OS tuning previously observed in the ON-OFF DSGCs. Together, these results not only confirm the role for Cx36 in mediating distal excitatory responses but also suggest that the Cx36 knockout is disrupting the OS tuning in other types of BCs or the other BCs in the circuit are not tuned for stimulus orientation.

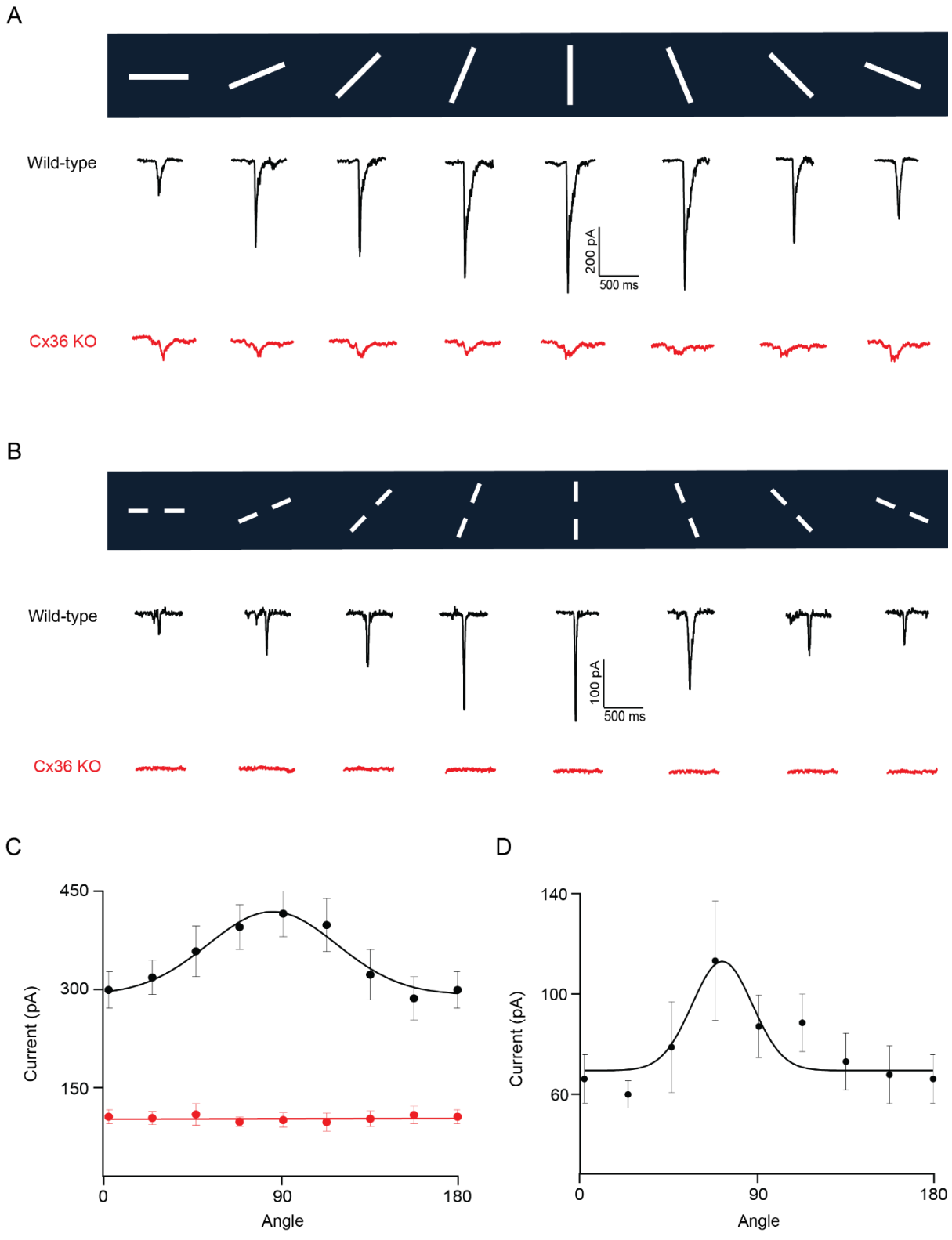
A
Wild-type
200 pA
500 ms
Cx36 KO
B
Wild-type
100 pA
500 ms
Cx36 KO
C
450
300
150
Current (pA)
0
90
180
Angle
D
140
100
60
Current (pA)
0
90
180
Angle

Figure 3.6 Glutamatergic excitation is tuned to the dorso-ventral axis of the retina

(A) Sample EPSC traces measured from a ventral coding DSGC obtained from a control retina (top; wild-type) for a stimulus flashing in 8 different orientations (n=8 cells; 1 – Dorsal; 4 – Ventral; 1 – Nasal; 2 – Temporal). Sample EPSC traces measured from a ventral coding cell obtained from a Cx36 KO retina (bottom; genetic knockout) for a stimulus flashing in 8 different orientations (n=5 cells). **(B)** Sample EPSC traces measured from a ventral coding DSGC obtained from a control retina (top; wild-type) for a static bar stimulus presented with a central occlusion (Mask size of 500µm) flashing in 8 different orientations (n=6 cells; 1 – Dorsal; 2 – Ventral; 1 – Nasal; 2 – Temporal). Sample EPSC traces measured from a ventral coding DSGC obtained from a Cx36 KO retina (bottom; genetic knockout) for a static bar stimulus presented with a central occlusion (Mask size of 500µm) flashing in 8 different orientations (n=5 cells). **(C)** Averaged peak EPSCs during 8 orientation stimulation (0 to 180◦ in increments of 22.5◦) in wild-type vs Cx36 KO retinas (Black – wild-type; Red – Cx36 KO). Data shown as mean ±SEM. **(D)** Averaged peak EPSCs during 8 orientation stimulation with central occlusion in wild-type vs Cx36 KO retinas (Black – wild-type; Red – Cx36 KO). Cx36 KO retinas did not generate any EPSCs. Data shown as mean ±SEM.

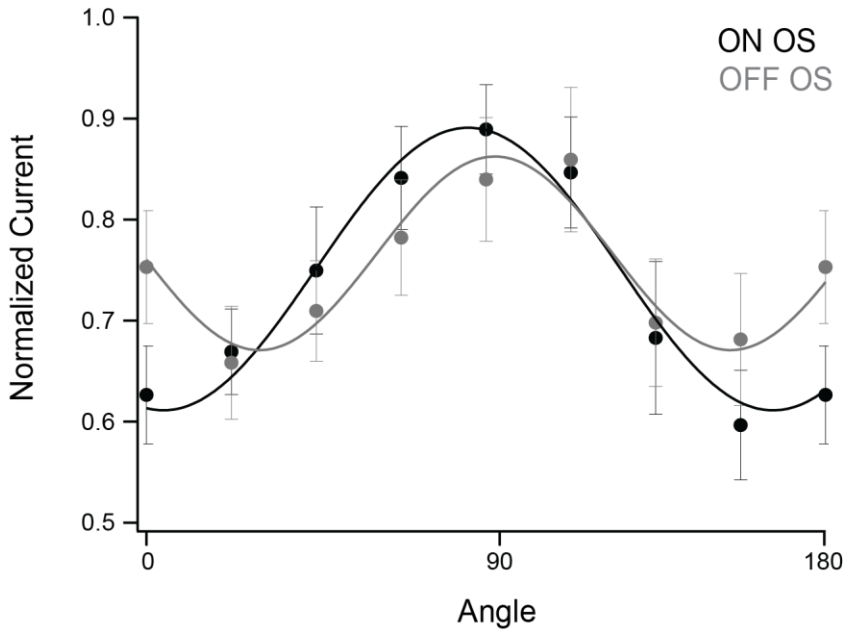

Figure 3.7 EPSC OS in all 4 types ON-OFF DSGCs

Normalized OS tuning curves for both ON and the OFF EPSC responses (n = 8) in the presence of inhibitory blockers (SR, TPMPA, and Hex). The responses are normalized to the peak current for both ON and OFF EPSCs.

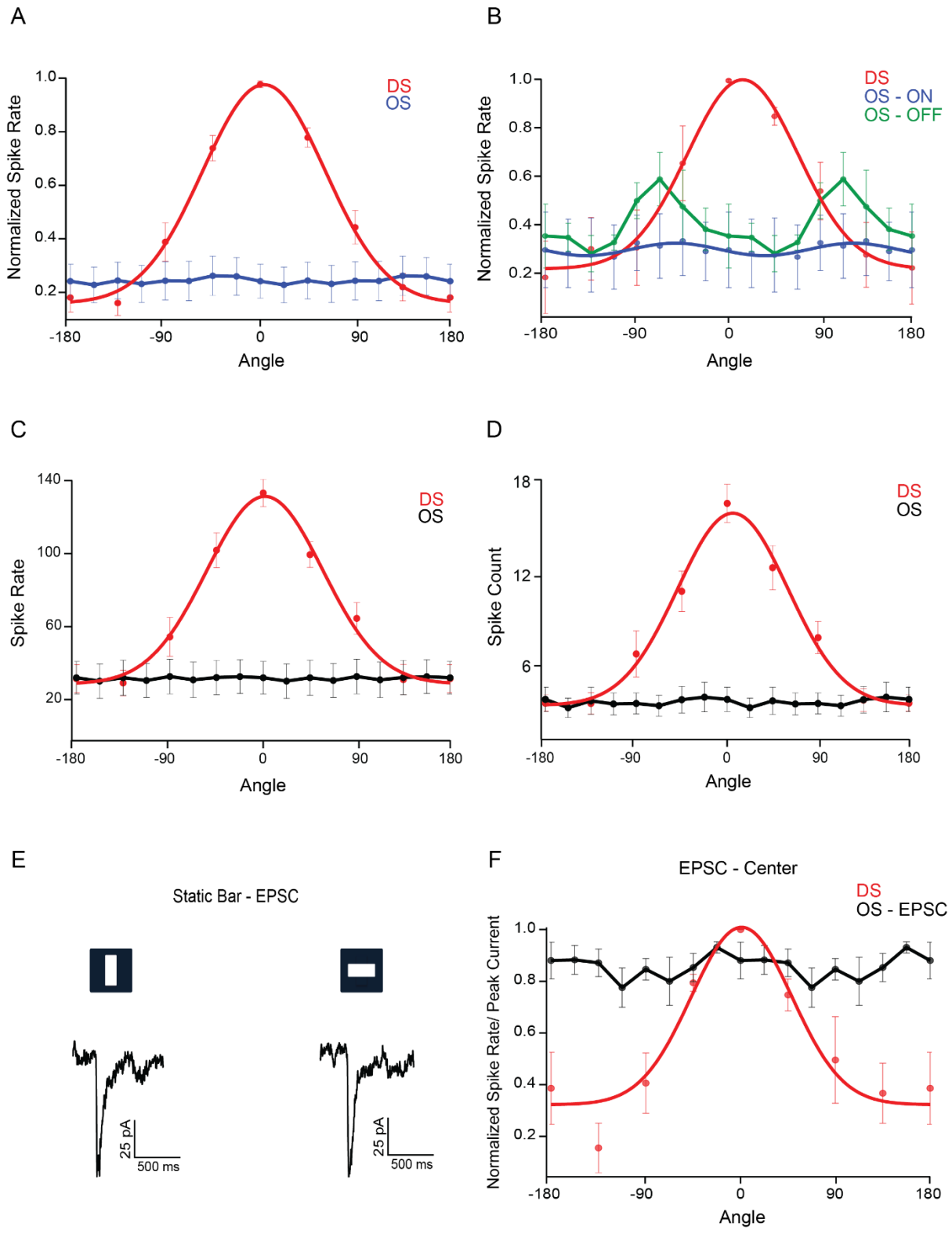
A
Normalized Spike Rate
1.0
0.8
0.6
0.4
0.2
DS
OS
-180
-90
0
90
180
Angle
B
Normalized Spike Rate
1.0
0.8
0.6
0.4
0.2
DS
OS - ON
OS - OFF
-180
-90
0
90
180
Angle
C
Spike Rate
140
100
60
20
DS
OS
-180
-90
0
90
180
Angle
D
Spike Count
18
12
6
DS
OS
-180
-90
0
90
180
Angle
E
Static Bar - EPSC
25 pA
500 ms
25 pA
500 ms
F
EPSC - Center
Normalized Spike Rate/ Peak Current
1.0
0.8
0.6
0.4
0.2
DS
OS - EPSC
-180
-90
0
90
180
Angle

Figure 3.8 – DS and OS tuning in Cx36 KO retinas

(A) Normalized DS and OS tuning curves constructed from the spiking responses recorded from ON-OFF DSGCs in the Cx36 KO (n=21 cells). **(B)** Normalized DS, OS ON, and OS OFF tuning curves constructed from the spiking responses recorded from ON-OFF DSGCs in the Cx36 KO. In KCng4-Cre Cx36 KO retinas, ON responses to large stationary stimuli are lost (ON OS, blue), while the OFF responses remain intact (OFF OS, green). Robust ON responses can be evoked using moving stimuli (DS<, red), indicating the specificity of the Cx36 KO to the BC5A (n=5). **(C)** Averaged spike rate traces for both DS and OS responses obtained from ON-OFF DSGCs in the Cx36 KO (n=21 cells). **(D)** Averaged spike count traces for both DS and OS responses obtained from ON-OFF DSGCs in the Cx36 KO (n=21 cells). **(E)** Sample EPSC traces from a ventral coding DSGC for both preferred orientation (PO) and null orientation (NO) of a static bar obtained from a Cx36 KO retina (n=5 cells). **(F)** Normalized EPSC tuning curves showing DS and OS tuning in Cx36 KO retinas (n=5 cells)

3.3 Optogenetic stimulation of BC5As reveal an orientation selective preference along the dorso-ventral axis of the retina

Further support for the idea that BC5A play a central role in shaping vertically tuned excitation came from optogenetic experiments. Previous studies have shown that optogenetic strategies can be used to stimulate SACs in transgenic mice in which channelrhodopsin (ChR2) is selectively expressed and can be used to measure monosynaptic responses in DSGCs in pharmacological isolation (Sethuramanujam et al., 2016). To provide concrete evidence that BC5As are responsible for conferring vertically tuned excitation in all 4 types of ON-OFF DSGCs, a double floxed ChR2 expressing genetic mouse line was crossed with KCNG4^{Cre} mouse line, which is shown to express BC5A (Type 5A BCs, also referred to as BP5i) along with a few others (Type 5B, C and X etc.,) which are sparsely distributed (Duan et al., 2014, Greene et al., 2016), and a few ganglion cells. BC5As expressed in KCNG4^{Cre}-ChR2 make up a significant majority of the BCs making synaptic contacts with all 4 types of ON-OFF DSGCs (Duan et al., 2014) has the light sensitive protein ChR2 predominantly in the BC5A and a few types of ganglion cells.

Firstly, to test if the ChR2 expression in the $Kcng4^{Cre}$ x $ChR2^{fl/fl}$ is strong enough to drive bipolar cell output, experiments were designed where ON-OFF DSGCs were identified and targeted under pharmacological isolation. To examine the functional properties of BC5A that drive the ON-OFF DSGC circuit in the mouse retina, the photoreceptor to bipolar cell transmission was blocked using metabotropic glutamate receptor agonist L-AP4 (L-2-amino-4-phosphonobutyric acid) and a kainite receptor antagonist (UBP310). To drive the activity in the BC5As, the stimulus intensity was increased 1000-fold (R*/s) to directly activate bipolar cells-expressing channelrhodopsin2 (ChR2) in relative isolation using a test spot (Figure 3.10A).

A cocktail of inhibitory blockers, including a $GABA_A$ receptor antagonist Gabazine (SR95531), $GABA_C$ receptor antagonist TPMPA ((1,2,5,6-Tetrahydropyridin-4-yl) methylphosphinic acid) and a nicotinic receptor antagonist Hexamethonium were added to the perfusion system. Once these drugs were washed in, electrodes filled with cesium and QX were used to voltage clamp the ON-OFF DSGCs. Experiments were performed to characterize the output response generated from DSGCs to confirm that glutamate release from BC5As is mediated by both AMPA and NMDA receptors (Figure 3.9). The cells were held at -30mV to remove the Mg^{2+} ion blocking the NMDA receptors. At -30mV, glutamatergic EPSCs mediated by both AMPA, and NMDA receptors were elicited with static bar stimuli 100 x 1200 µm or 200 x 1200 µm with varying mask sizes ranging from 300 µm in diameter all the way up to 900 µm flashing in 8 different orientations. These masks were used in the middle of the bar to occlude the center and stimulate the surround, thereby targeting the BC5A which are thought to be present at the farthest end, making synaptic contacts with WACs as shown in the schematic. Most strikingly, excitatory signals could be evoked with remote stimuli in all types of DSGCs, as long as the stimuli were placed along the vertical axis (Figure 3.10B). This way of stimulating BC5A by presenting stimuli outside of the receptive field of these BCs potentially requires another synaptic partner, possibly one

with long-range lateral connections (Hanson et al., 2023). The EPSCs measured from bars with a central mask of varying sizes were all tuned to the vertical orientation (Figure 3.10C).

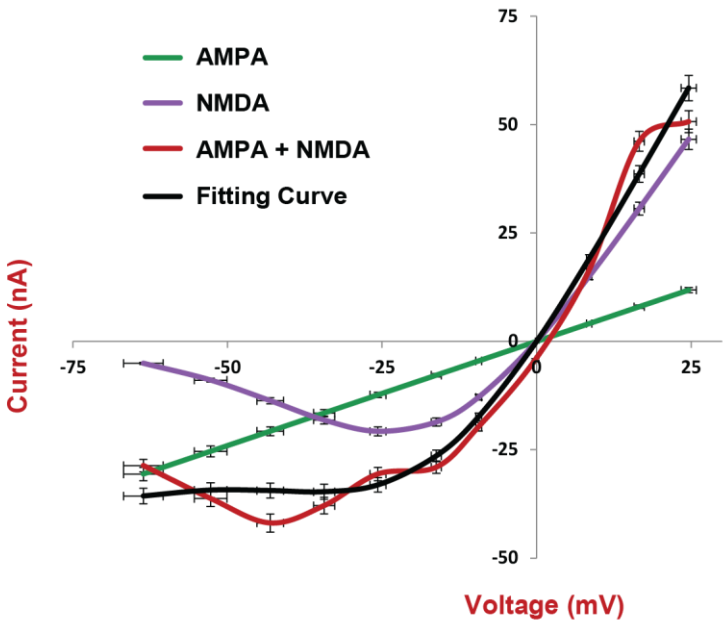

Figure 3.9 – I-V relationship measuring glutamatergic contribution mediated by AMPA/NMDA receptors

Current (nA) plotted as a function of holding potential (mV), constructed from a ventral coding ON-OFF DSGC obtained from a KCNG4Cre-ChR2 retina (n=4 trials). Ach – Acetylcholine; AMPA – Alpha-amino-3-hydroxy-5-Methyl-4-isoxazole Propionic Acid; NMDA – N-Methyl-D-Aspartate; GABA – Gamma-Amino Butyric Acid.

This is in line with what has been observed in wild type mice models, where the distal excitation was shown to be tuned to the vertical axis (dorso-ventral axis of the retina). These results provide further evidence for the role of BC5A in generating vertically tuned excitation across the different populations of DSGCs. They also help consolidate previous SBEM analysis demonstrating that BC5A are reciprocally coupled with WF5A through mixed glutamatergic/electrical synapses (Hanson et al., 2023).

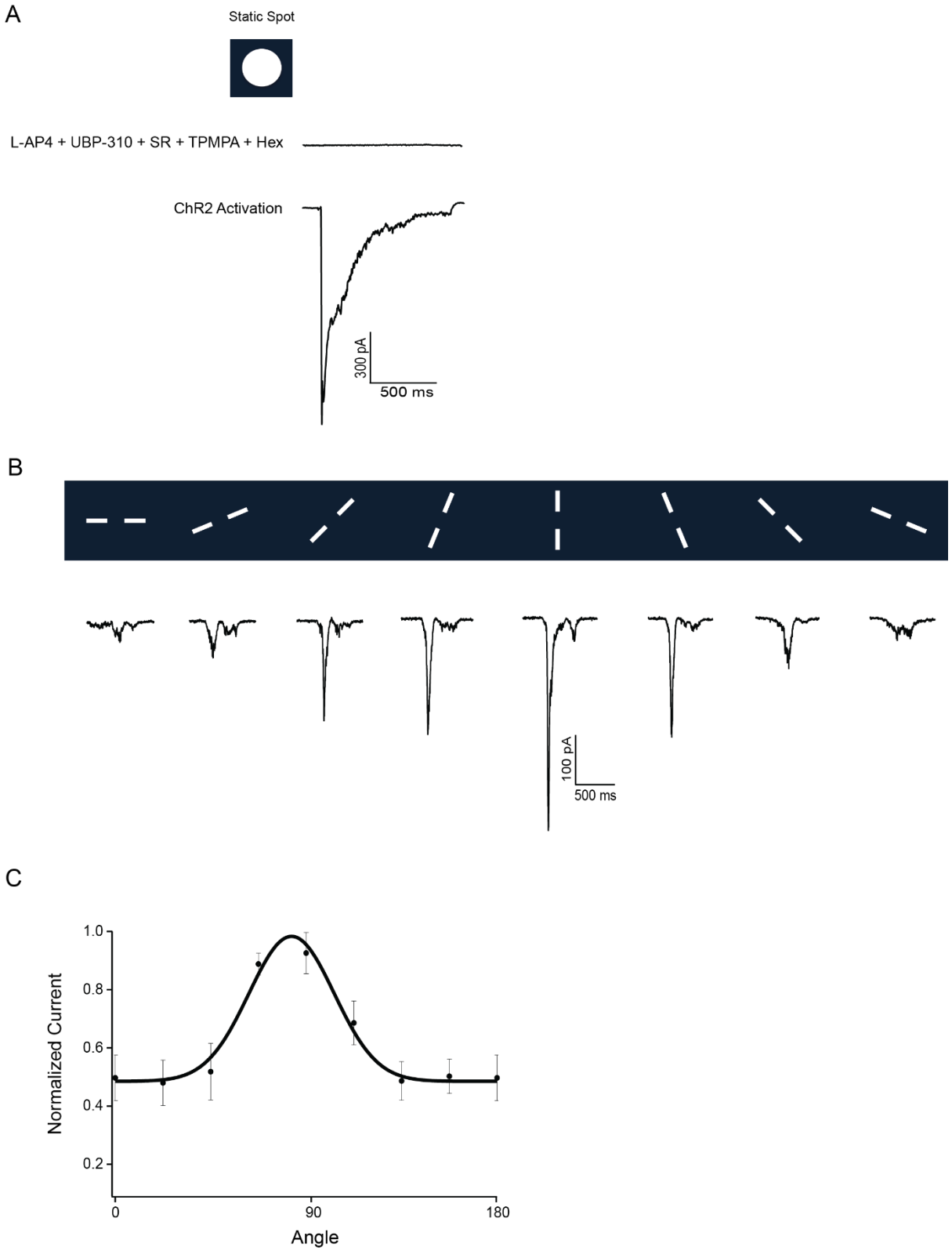
A
Static Spot
L-AP4 + UBP-310 + SR + TPMPA + Hex
ChR2 Activation
300 pA
500 ms
B
100 pA
500 ms
C
Normalized Current
1.0
0.8
0.6
0.4
0.2
0
90
180
Angle

Figure 3.10 Distal BC5A stimulation using ChR2 reveals dorso-ventrally tuned excitation to all DSGCs

(A) Sample EPSC response for a static spot of 200µm in size when synaptic transmission between photoreceptors and bipolar cells are blocked and during channelrhodopsin (ChR2) stimulation. **(B)** Sample EPSC traces measured from a dorsal coding DSGC obtained from $Kcng4^{Cre}$ x $ChR2^{fl/fl}$ retina for a static bar stimulus presented with a central occlusion (600µm mask) flashed in 8 different orientations (n=7 cells). **(C)** Normalized peak EPSCs for a static bar stimulus presented with a central occlusion (Mask size of 600µm) flashing in 8 different orientations in $Kcng4^{Cre}$ x $ChR2^{fl/fl}$ retinas (n=7 cells; 1 – Dorsal; 2 – Ventral; 3 – Nasal; 1 – Temporal). Data shown as mean ±SEM.

3.4 Orientation-selective inhibition aligns with the preferred-null axis of the ON-OFF DSGCs

The mismatch between the glutamatergic input and spiking output tuning properties observed for DV coding DSGCs suggest that other important factors are involved in shaping orientation selectivity. Asymmetric inhibition from the starbursts is most obvious choice of mechanisms, given their asymmetric wiring provides maximum inhibition along the null direction of the ON-OFF DSGCs provided by SACs (Figure 3.11A; Trenholm et al., 2011). However, starburst amacrine cells are usually activated by moving stimuli, and the extent to which they are activated by static bars and contribute to orientation selectivity is unclear. To test whether starburst inhibition could play a role in generating orientation selectivity I next measured the IPSCs in DSGCs voltage clamped at 0 mV (reversal for excitation), evoked by static bars.

Consistent with their role in driving direction selectivity, large IPSCs were evoked when bars moved across the DSGC's receptive field in the null direction. By contrast, IPSCs evoked by static bars were relatively weak in comparison (Figure 3.11B, C). Nevertheless, IPSCs were tuned for stimulus orientation. In contrast to the tuning of BC input, maximum inhibition was evoked by bars that were

oriented along the DSGC's PN axis. This pattern of inhibition suggest that starbursts could also play a role in shaping OS in DSGCs.

Next, to test whether starburst inhibition can shape orientation selectivity in DSGCs, I resorted using an optogenetic approach. Consistent with previous studies, I found that directly activating starbursts using ChR2 (Chat-Cre x Ai32) with moving bars evoked robust DS responses in DSGCs, even after photoreceptor synapses were blocked (Figure 3.11E, G; DS – red traces). Under these pharmacological conditions, DSGCs cells are driven by a mixture of GABAergic inhibition and cholinergic excitation both arising from starburst amacrine cells (Sethuramanujam et al., 2016).

Interestingly, robust orientation selectivity was also apparent in all types of DSGCs when they were stimulated by static bars (Figure 3.11D, F). Similar to control conditions, the orientation selectivity observed in the extracellular spiking was orthogonal to the DSGC's PN axis (Figure 3.11E). As expected, the orientation tuning in IPSCs were aligned to the P-N axis of the DSGCs (Figure 3.11G). Results from these experiments demonstrate the potential for the starburst network alone to drive both OS and DS responses.

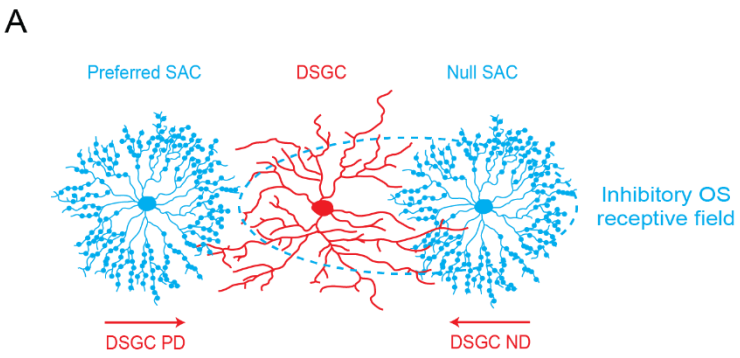
A
Preferred SAC
DSGC
Null SAC
Inhibitory OS
receptive field
DSGC PD
DSGC ND

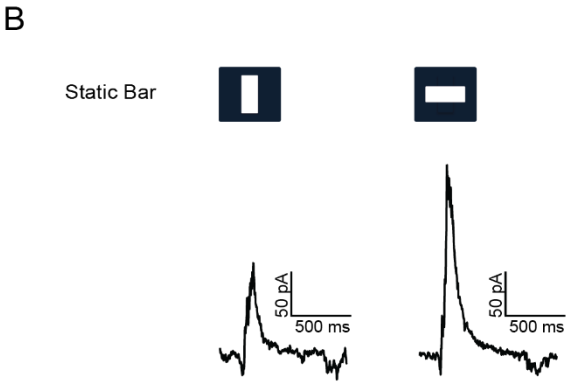
B
Static Bar
50 pA
500 ms
50 pA
500 ms

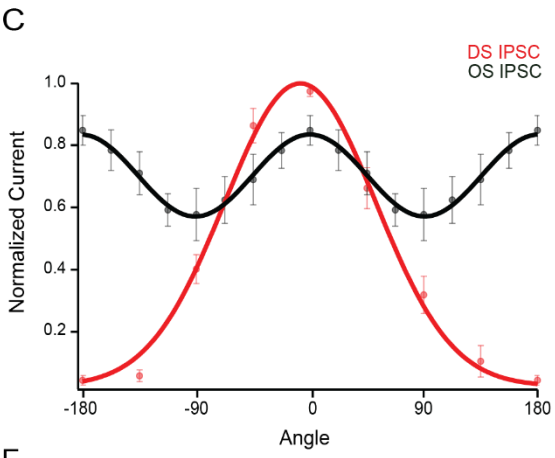
C
DS IPSC
OS IPSC
Normalized Current
1.0
0.8
0.6
0.4
0.2
-180
-90
0
90
180
Angle

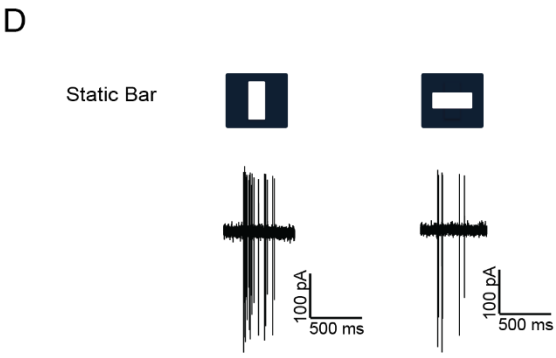
D
Static Bar
100 pA
500 ms
100 pA
500 ms

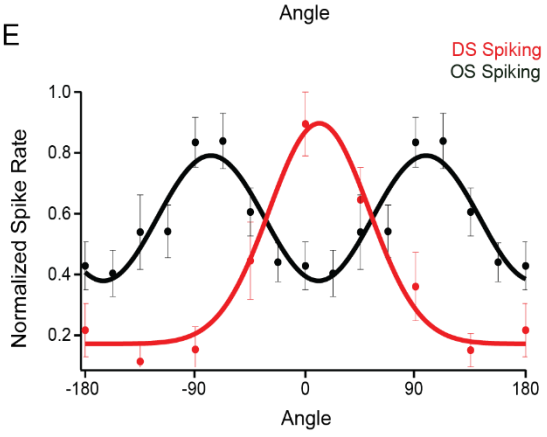
E
DS Spiking
OS Spiking
Normalized Spike Rate
1.0
0.8
0.6
0.4
0.2
-180
-90
0
90
180
Angle

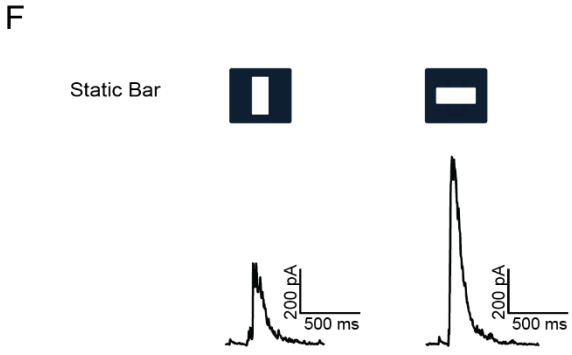
F
Static Bar
200 pA
500 ms
200 pA
500 ms

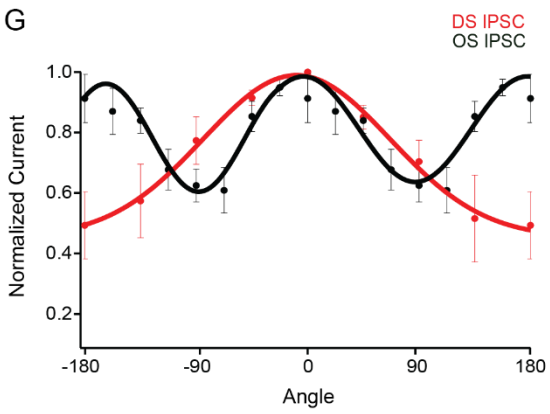
G
DS IPSC
OS IPSC
Normalized Current
1.0
0.8
0.6
0.4
0.2
-180
-90
0
90
180
Angle

Figure 3.11 OS inhibition is tuned to the P-N axis of the ON-OFF DSGCs

(A) Illustration showing DSGC-SAC network with inhibitory OS receptive field aligned with the null SAC. **(B)** Sample IPSC traces from a nasal coding DSGC for both preferred orientation (PO) and null orientation (NO) of a static bar. **(C)** Normalized spike rate/current tuning curves showing DS and OS IPSC fitted with a gaussian function (n=9; 1 – Dorsal; 5 – Ventral; 1 – Nasal; 2 – Temporal). **(D)** Sample spiking traces from a ventral coding DSGC for both preferred orientation (PO) and null orientation (NO) of a static bar obtained from a ChAT-cre-ChR2 retina (n=7 cells; 1 – Dorsal; 2 – Ventral; 2 – Nasal; 2 – Temporal). **(E)** Normalized spike rate tuning curves showing DS and OS tuning in ChR2 (n=7). **(F)** Sample IPSC traces from a ventral coding DSGC for both preferred orientation (PO) and null orientation (NO) of a static bar obtained from a ChAT-cre-ChR2 retina (n=5 cells; 1 – Dorsal; 2 – Ventral; 2 – Nasal). **(G)** Normalized IPSC tuning curves showing DS and OS tuning in (n=5 cells).

3.5 Orientation selectivity in D/V– vs. N/T– coding DSGCs rely on distinct mechanisms

So far, the voltage-clamp analysis has shown that for NT-coding DSGCs, the excitatory and inhibitory inputs exhibit complementary tuning patterns. Specifically, the stronger spiking response to vertical bars is associated with large glutamatergic excitation and weak GABAergic inhibition, while the weak responses to horizontal bars with weak excitation and strong inhibition as shown in. However, for the DV coding DSGCs, the excitatory and inhibitory mechanism appear to converge at multiple levels. OS excitation to vertical dendrites of starburst produce a stronger inhibitory output. At the level of DSGCs, the sign-inversion by starburst appears to lead to cancellation of vertically tuned BC excitation. Thus, the preferred spiking responses of DV coding DSGCs are likely to be associated with weaker excitation and inhibition.

However, since the excitatory inputs were measured under GABA receptor blockade, which potentially could have affected the tuning patterns themselves, in a final set of experiments I tested how the tuning properties of the DSGCs are affected when starburst output was selectively blocked using a metabotropic glutamate receptor 2,3 agonist (mGluR2,3 agonist; 10 µM DCG-IV; Sethuramanujam et al., 2018). mGluR2s are expressed selectively by starbursts and have thus been a valuable tool to selectively manipulate starburst activity (Nakanishi et al., 2001). 10 µM of DCG-IV was washed on to the perfusion system to render the SACs inactive. The bath application of DCG-IV increased the spike rate (Figure 3.12B) and led to a loss of direction selectivity in all types of DSGCs Figure (3.12C-D), consistent with the expected outcomes of removing starburst inhibition. However, the effects of DCG-IV on orientation selectivity were cell-type specific. For NT coding DSGCs, DCG-IV did not significantly alter the OS tuning curve, as previously reported (Hanson et al., 2023; Figure 3.12F). Orientation selectivity was also apparent in DV coding DSGCs after blocking starburst output. However, under these conditions the preferred orientation was no longer orthogonal to the DSGCs PN axis. The dorsal and ventral coding ON-OFF DSGCs were responding maximally to a bar oriented along their preferred-null axis, which is in contrast to what was observed in control conditions. This vertically tuned extracellular spiking response was parallel to the PN axis, similar to BC input tuning. Thus, rendering the SACs inactive does not remove orientation selectivity but appears to ‘flip’ the orientation preference in these DSGCs (Figure 3.12E). Together these results lead us to conclude that the OS tuning of DV-coding but not NT coding DSGCs critically relies on starburst inhibition.

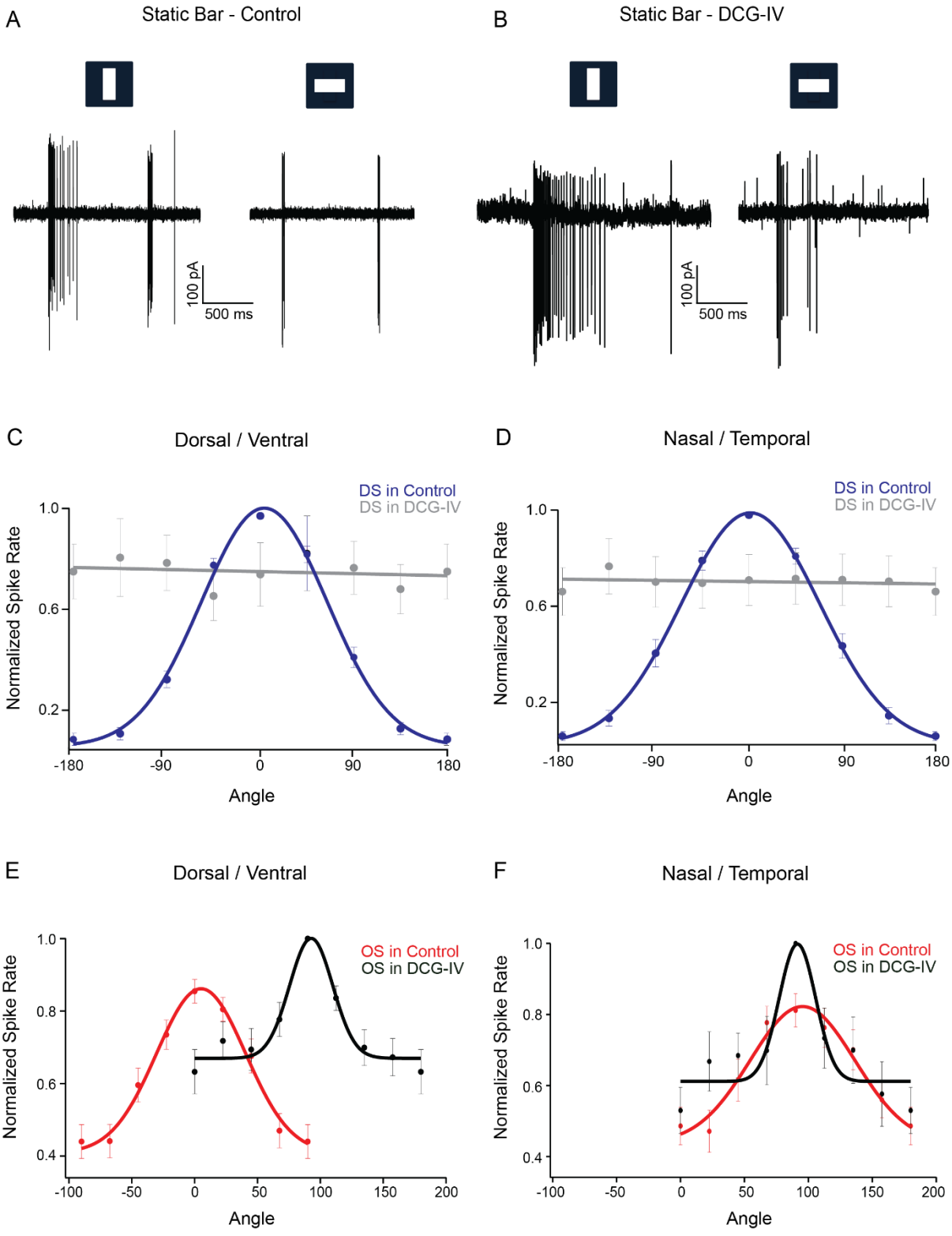
A
Static Bar - Control
100 pA
500 ms
B
Static Bar - DCG-IV
100 pA
500 ms
C
Dorsal / Ventral
DS in Control
DS in DCG-IV
Normalized Spike Rate
1.0
0.6
0.2
-180
-90
0
90
180
Angle
D
Nasal / Temporal
DS in Control
DS in DCG-IV
Normalized Spike Rate
1.0
0.6
0.2
-180
-90
0
90
180
Angle
E
Dorsal / Ventral
OS in Control
OS in DCG-IV
Normalized Spike Rate
1.0
0.8
0.6
0.4
-100
-50
0
50
100
150
200
Angle
F
Nasal / Temporal
OS in Control
OS in DCG-IV
Normalized Spike Rate
1.0
0.8
0.6
0.4
-100
-50
0
50
100
150
200
Angle

Figure 3.12 Orientation selectivity in D/V coding DSGCs 'flips' when SAC output is abolished

(A) Sample extracellular spiking traces from a ventral coding DSGC for both preferred orientation (PO) and null orientation (NO) of a static bar obtained from a wild-type (control) retina (n=117 cells). **(B)** Sample extracellular spiking traces from a ventral coding DSGC for both preferred orientation (PO) and null orientation (NO) of a static bar obtained from a wild-type (control) retina perfused with DCG-IV (n=46 cells). **(C)** Normalized DS tuning curves for both control (n=71 cells) and DCG-IV (n=31) conditions obtained from dorsal and ventral coding DSGCs. **(D)** Normalized DS tuning curves for both control (n=46 cells) and DCG-IV (n=15) conditions obtained from nasal and temporal coding DSGCs. **(E)** Normalized OS tuning curves for both control (n=71 cells) and DCG-IV (n=31) conditions obtained from dorsal and ventral coding DSGCs showing 'Flip'. **(F)** Normalized OS tuning curves for both control (n=46 cells) and DCG-IV (n=15) conditions obtained from nasal and temporal coding DSGCs. In graphs E and F, the normalized control peak isn't at 1 because there are slight differences in the preferred orientation angle of these cells, and they get averaged.

3.6 Vertically tuned excitation contributes to the differences in DS tuning width between horizontally and vertically oriented motion

Various measures have been proposed for assessing the strength and sharpness of DS tuning for a given neuron (Henry et al., 1974; De Valois et al., 1982; Weng et al., 2005). Directional tuning curves plotted from the synaptic response of DSGCs are typically quantified based on a direction-selective index (DSI). Traditionally, for the purpose of measuring DS, spots and bars of varying sizes and drifting gratings have been used. In order to understand how DS tuning width is affected by stimulus size and shape, spike responses from DSGCs using bars oriented along two different axes (i.e., horizontal, and vertical axes) were measured. For these experiments a long bar is moved parallel to the long axis of the bar. Wide bar moves perpendicular to the long axis of the bar. The spiking responses of DSGCs to a long bar (600 x 100 µm) and a wide bar (100 x 600 µm) moving in 8 directions (velocity 1600 µm/s) were measured. The sample spiking traces for both orientations of a bar are shown in the (Figure 3.14A, B). The DS responses obtained for different stimulus types from these ON-OFF DSGCs varied in strength (based on DSI measurements). For a wide bar, the DS tuning was sharp (little to no spiking

along the null directions) and narrow as shown in the (Figure 3.13A, B). The average DSI of the tuning curve was high (DSI ~ 0.55). Whereas, for a long bar (a bar oriented along the horizontal axis to the field of view of the retina), the DS tuning was wider (null directional spike rate was higher than that of the wide bar) and the average DSI of the tuning curve was lower than that of the wide bar (DSI ~ 0.35). I hypothesize that the differences in DS tuning width between both a wide bar and a long bar exists as a result of the asymmetric surround excitation. The tuning curves obtained from all four types of DSGCs, for both a wide bar and a long bar were fitted with a Von Mises distribution and the concentration (κ) values for both a wide bar and a long bar were calculated (Lockhart & Stephens, 1985) (Figure 3.13C-F).

In a given Von Mises distribution, the lower the κ value, the more uniform the distribution of variables within a given data set, and the differences in κ values between a wide bar and a long bar indicate that both the data sets are non-uniform. The vertically tuned excitation received from the BC5As could be contributing to the differences in DS tuning width between a horizontal vs vertical bar. It is also possible that ON-OFF DSGCs prefer an optimal stimulus type (size and shape) for which maximum response amplitude can be achieved. Considering that DS tuning widths have been shown to be stimulus dependent (Fiscella et al., 2015; it can be inferred that certain asymmetries arising from the stimulus shape and size causes there to exist a preference for certain orientations to favor maximum spike generation over others. These results indicate that there could be an intrinsic bias within the DSGC circuit for an optimal stimulus (specific size and shape) to which they elicit maximal response. The circuit connections between presynaptic BC5As with asymmetrically distributed WAC dendrites adds credibility to the idea that ON-OFF DSGCs prefer an optimal stimulus which produces maximum spike output.

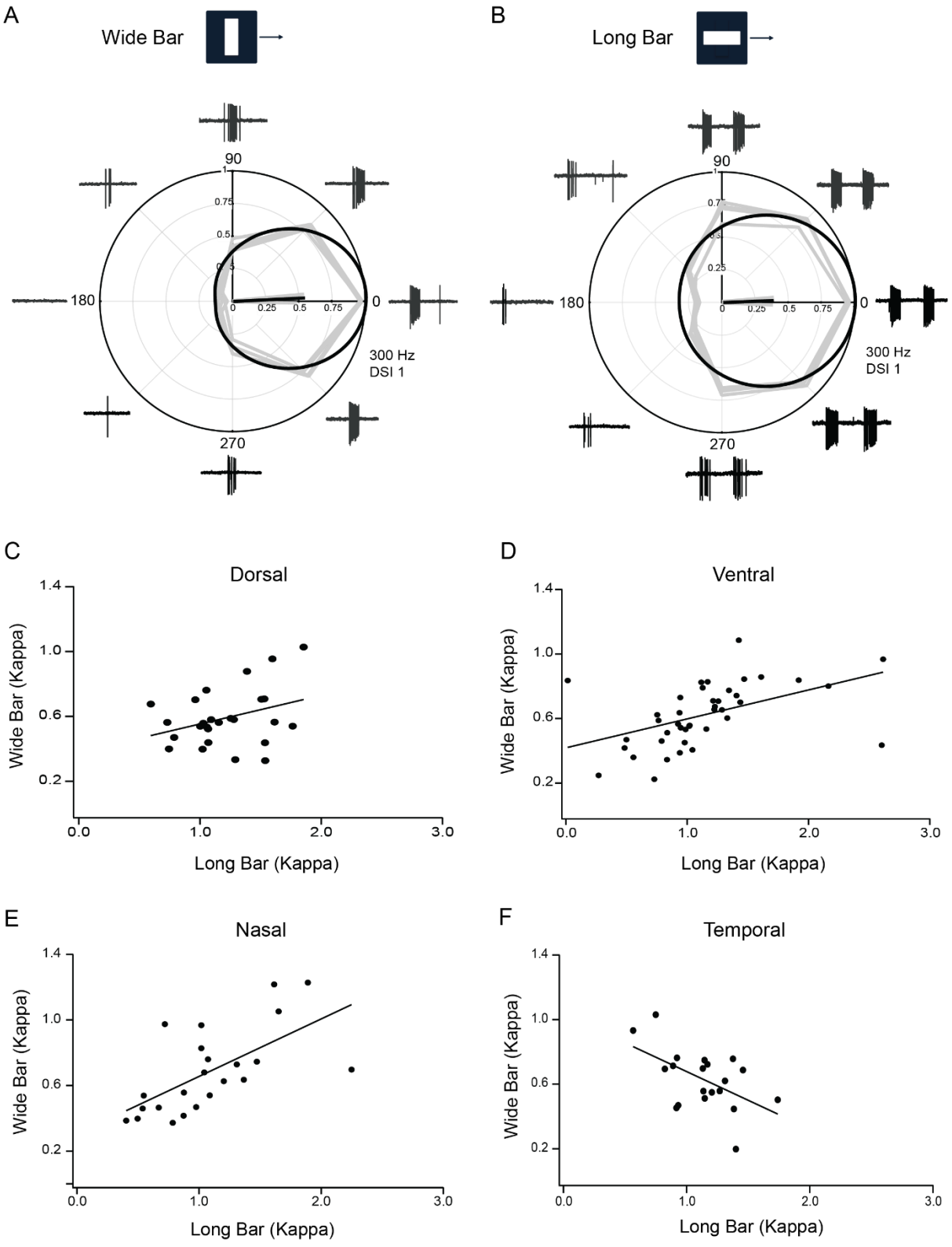
A
Wide Bar
90
180
0
270
300 Hz
DSI 1
B
Long Bar
90
180
0
270
300 Hz
DSI 1
C
Dorsal
Wide Bar (Kappa)
Long Bar (Kappa)
D
Ventral
Wide Bar (Kappa)
Long Bar (Kappa)
E
Nasal
Wide Bar (Kappa)
Long Bar (Kappa)
F
Temporal
Wide Bar (Kappa)
Long Bar (Kappa)

Figure 3.13 DS tuning differences for wide vs long bars

(A) Normalized average DS tuning for a wide bar obtained from all 4 types of DSGC represented as a polar graph calculated from the peal spike rate during 8 direction stimulation with spiking responses normalized to the DS peak angle to be along 0° shown across the polar graph (Grey = individual trials, Black = average; n=117). DSI – Direction selectivity index, measured as the vector sum of the responses in all 8 direction. **(B)** Normalized average DS tuning for a long bar obtained from all 4 types of DSGC represented as a polar graph calculated from the peal spike rate during 8 direction stimulation with spiking responses normalized to the DS peak angle to be along 0° shown across the polar graph (Grey = individual trials, Black = average; n=117). DSI – Direction selectivity index, measured as the vector sum of the responses in all 8 direction. **(C)** Paired scatter plot represented as a function of concentration (κ) for wide vs long bars obtained from all dorsal coding DSGCs (n=30). **(D)** Paired scatter plot represented as a function of concentration (κ) for wide vs long bars obtained from all ventral coding DSGCs (n=41). **(E)** Paired scatter plot represented as a function of concentration (κ) for wide vs long bars obtained from all nasal coding DSGCs (n=25). **(F)** Paired scatter plot represented as a function of concentration (κ) for wide vs long bars obtained from all temporal coding DSGCs (n=21).

4. Discussion

Previous work studying retinal circuits have only described two separate circuit mechanisms for conveying direction and orientation information. In this study I demonstrate that multiple network mechanisms drive OS responses in ON-OFF DSGCs. Manipulating the presynaptic BC contacts revealed that type 5A bipolar cells (BC5A) provide vertically-tuned glutamate input to all four types of DSGCs, a feature that relies on Cx36 containing gap junctions. However, different types of DSGCs seem to respond best to either horizonal or vertical bars that are orthogonal to their preferred directions. Following this, selective ablation of SACs revealed that for DV-coding DSGCs (dorsal and ventral coding populations) the vertically-tuned excitation is effectively dominated by the starburst network, thereby 'flipping' the DSGC's preferred orientation. Thus, distinct combinations of inhibition and excitation appear to underlie orientation selectivity in the nasal/temporal and dorsal/ventral coding DSGC populations, the latter critically relying on the starbursts.

4.1 Multiplexing direction and orientation information in the population of ON-OFF DSGCs

Both excitatory and inhibitory inputs appear to shape the OS responses evident in ON-OFF DSGCs and this relies on three transmitter systems: glutamate from BCs and GABA/ACh from starbursts. For all 4 types of ON-OFF DSGCs, the postsynaptic spiking responses to OS stimulus measured were orthogonal to its P-N axis of motion (Figure 3.2F). This phenomenon has previously been described in the visual cortex where DS neurons are also tuned for stimulus orientation. Both excitatory and inhibitory inputs have been shown to be involved in establishing the tuning preference of these cortical neurons (Hubel & Wiesel, 1959, 1962, Weliky et al., 1996; Monier et al., 2003; Priebe &

Ferster, 2005). The specific morphology of the presynaptic contacts and co-tuned excitatory connections arising from various layers of the visual cortex have been shown to contribute to this dual feature selectivity seen in the cortical neurons (Rossi et al., 2020). Contrary to what has been observed in cortex, researchers have only reported directional signals from the retinal DS circuit, possibly because the directional signals it sends to the brain are so salient, and the presynaptic circuitry is so specifically arranged as to enable that selectivity.

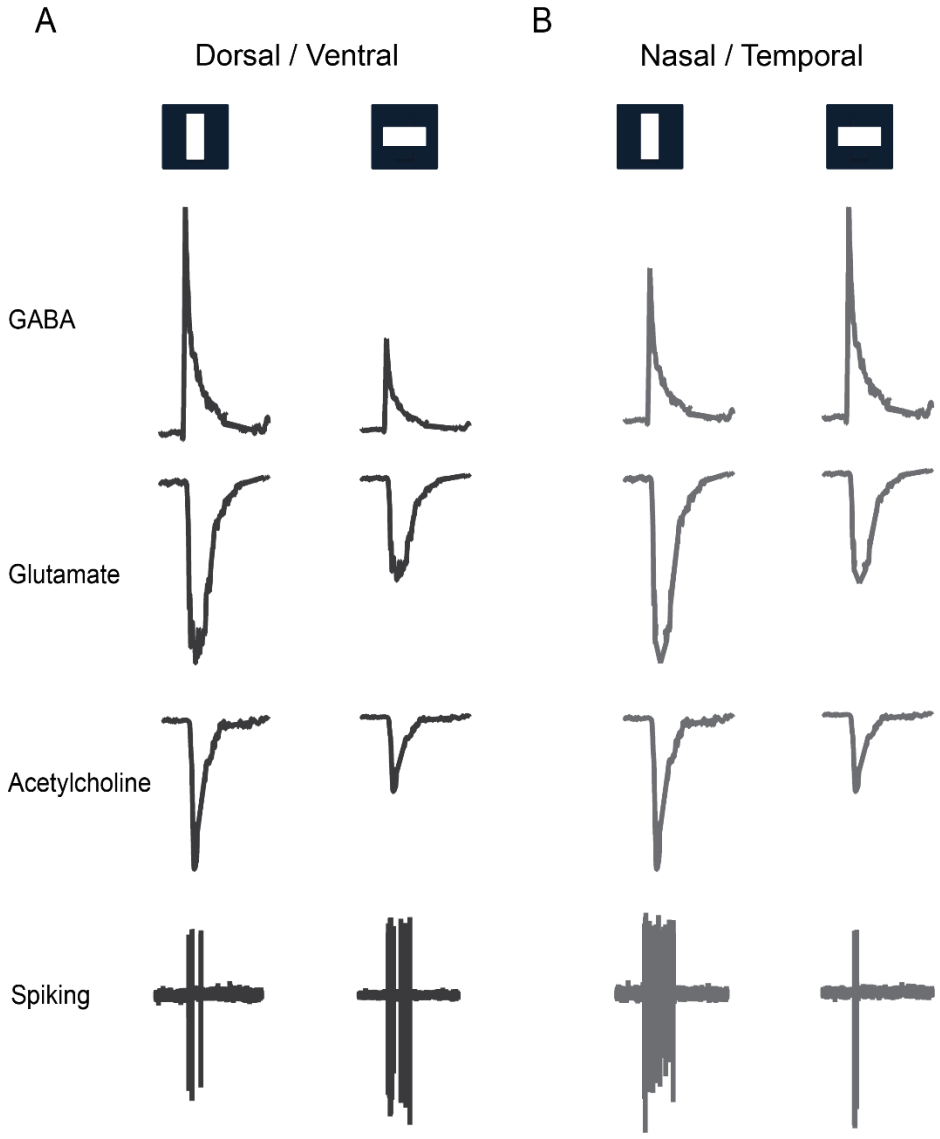

Figure 4.1 – Sample sketch of the presynaptic inputs to D/V and N/T coding cells

(A) Sample traces for GABA, glutamate, Ach, and post-synaptic spiking for D/V coding DSGCs for both preferred orientation (PO) and null orientation (NO) of a static bar. **(B)** Sample traces for GABA, glutamate, Ach, and post-synaptic spiking for N/T coding DSGCs for both PO and NO of a static bar. Ach – Acetylcholine; GABA – Gamma-Amino Butyric Acid.

Previous studies have shown that orientation selectivity observed in OSGCs arises because of the dendritic morphology of the OS neurons, asymmetric excitation from the presynaptic bipolar cells and inhibitory OS arising from the presynaptic amacrine cell contacts (Levick 1967; Venkataramani & Taylor, 2010, 2016; Nath & Schwartz, 2016, 2017). Decades of research findings also support the claim that a variety of inhibitory amacrine cells harbor dendritic processes that extend out along the horizontal or vertical axes, and this integration of information along a single axis gives rise to orientation selectivity (Hubel & Wiesel, 1962; Venkataramani & Taylor, 2010). Here I observe that BC5A-WF5A mediated glutamatergic excitation is tuned to the vertical axis of the retina for all 4 types of ON-OFF DSGCs. This could be because of the morphological bias of the synaptic amacrine cell contacts. BC5A axon terminals receive inputs from WF5As via Cx36 containing gap-junctions (Hanson et al., 2023). These WF5As have vertically elongated dendritic processes, that could potentially carry the glutamatergic excitation over long ranges along the vertical axis of the retina (Bloomfield et al., 1991, 1994; Murphy-Baum et al., 2015, Hanson et al., 2023). When these Cx36 containing gap-junctions are disrupted, all 4 types of ON-OFF DSGCs lose this vertical excitation.

It is interesting to see the loss of OS in the absence of BC5A and WF5A electrical connections. In a recently published study, it was shown that orientation selectivity relies on gap junctions (Hanson et al., 2023). The retina is enriched with gap junctions and long-range gap junction coupling between bipolar cells and other cell types have been previously described (Bloomfield and Völgyi, 2009). Specifically, the connexin 36-containing gap junctions have been implicated in BC5A connections to

WACs (Zhang and Wu, 2009; Hoggarth et al., 2015; Hanson et al., 2023). Given that BC axon terminals do not really extend over large areas (Chen et al., 2014), cells which have widespread dendritic processes might be electrically coupled to these presynaptic bipolar cells to mediate a response in the downstream ganglion cells.

We know that overlapping sets of BCs drive all four types of ON-OFF DSGCs (Helmstaedter et al., 2013; Duan et al., 2014; Ding et al., 2016), and so it is possible that only BC5As are tuned for the vertical orientation, and other BCs are tuned for the horizontal orientation or are not tuned for stimulus orientation. Since there is also loss of EPSC amplitude in addition to the loss of OS tuning in the responses obtained from Cx36 KO retinas, it can be inferred that vertical excitation from BC5As dominate the excitatory inputs provided to ON-OFF DSGCs. It is certainly more efficient to have a circuit mechanism where the same type of bipolar cell, i.e., BC5As provides vertical excitation to all 4 types of ON-OFF DSGCs and further modulate the other presynaptic partners to have different effects in the downstream DSGCs. This finding is in line with the results from a recent study which demonstrated that BC5As provide vertically tuned input to nasal coding TRHR+DSGCs, which were critical for generating their orientation selectivity (Hanson et al., 2023).

One caveat that I have addressed while designing this experimental setup is that, by means of including all inhibitory blockers to measure the glutamatergic contribution to bipolar cells, we are removing the possibility of disinhibition activating the WACs and the only remaining pathway through which these amacrine cells could be excited is electrically through glutamatergic excitation from their synaptic partners. These findings not only validate the role of Cx36 containing gap junctions in mediating distal excitation, but also add credibility to the idea that knocking out Cx36 containing gap junctions might disrupt the OS tuning in other types of BCs or the other BCs in the circuit are not tuned for stimulus orientation. These circuit specializations support the notion that in the mouse visual system

the vertical axis may represent a key reference axis along which visual information can be organized (Coppola et al., 1998). Nevertheless, results obtained from measuring glutamatergic excitation does not to explain the orthogonal relationship between DS and OS observed in the ON-OFF DSGCs. This opens the stage to multiple contributing factors potentially responsible for conferring OS tuning in downstream DSGCs.

Alternatively, it is possible that inhibition from starbursts drives OS in DSGCs. Starbursts are known to asymmetrically connect to DSGCs in a way that predicts that they would drive a stronger inhibition for bars placed along the DSGCs P-N axis (Figure 3.2B, F; Fried et al., 2002; Lee et al., 2010; Briggman et al., 2011; Yonehara et al., 2013; Chen et al., 2016; Brombas et al., 2017). Stimulating the P-N axis of the DSGCs would therefore produce large IPSC as opposed to the orthogonal axis. However, I found that the relative strength of inhibitory OS measured from D/V and N/T coding DSGCs were different in WT and ChR2 mediated conditions. In D/V coding DSGCs, GABAergic inhibitory OS measured from WT and ChR2 conditions were comparable. Although similar mechanisms for generation of IPSCs are involved in N/T coding DSGCs as well, stronger inhibitory OS was only evident in SAC-ChR2-evoked responses when compared to the WT conditions. This shows that there is a bias for stronger OS inhibition along the dorso-ventral axis of the retina. Although SACs have been previously implicated for their asymmetric preference only to moving stimuli, it is surprising to see that there exists a strong OS bias for static stimuli in both WT and ChR2 conditions.

One possible explanation for stronger inhibition along the P-N axis for the D/V coding cells is the stronger stimulation of BC5As along the vertical axis that in turn activates the SACs (Dual et al., 2014; Ding et al., 2016, Hanson et al., 2023). This strong SAC inhibition along the null direction (dorso-ventral axis of the retina) could in fact be masking the vertical OS excitation that D/V coding DSGCs receive from the BC5As (Figure 3.5B, C), suggesting an additive role for SACs in sharpening the OS

tuning in specific population of DSGCs. This is supported by experimental evidence showing that when SAC output is abolished in the presence of DCG-IV (Sethuramanujam et al., 2018), the postsynaptic spiking responses to OS stimulus obtained from the dorsal and ventral coding ON-OFF DSGCs flipped and were tuned to be along the dorso-ventral axis of the retina (Figure 3.13E). The other potential reason for the differential inhibitory OS tuning evident in D/V vs N/T coding DSGCs could be because of the action of other pre-synaptic amacrine cells which could be modulating the SAC output.

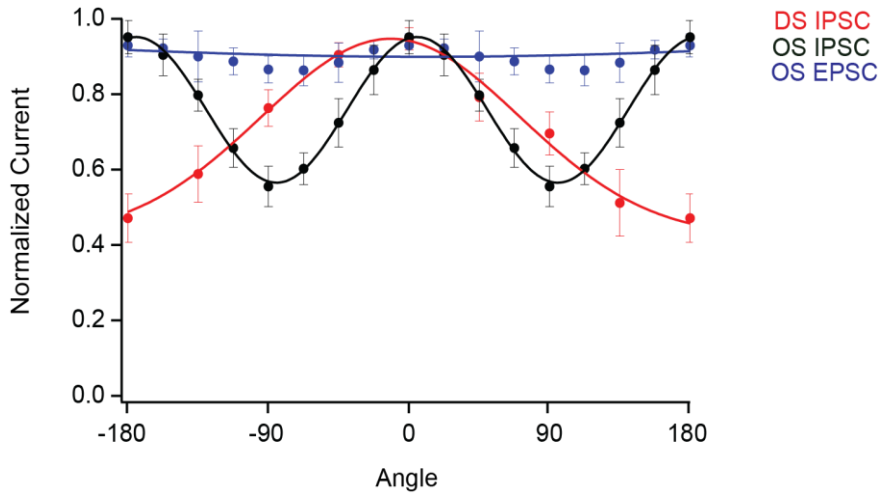

Figure 4.2 SAC-ChR2 mediated responses in ON-OFF DSGCs

Normalized IPSC and EPSC tuning curves showing DS and OS tuning in all 4 types of DSGCs (n=9 cells).

The asymmetry in wiring combined with the stronger activation of SACs along the dorso-ventral axis of the retina would be affecting ACh inputs and thus provide asymmetric cholinergic excitation to both D/V and N/T coding DSGCs (Figure 4.1). Direct evidence that the BC5As are differentially modulating the SAC inputs along the vertical axis of the retina was provided from the IPSCs and EPSCs obtained from SAC-ChR2 mouse line. Despite this asymmetry in the wiring, starburst excitation is

expected to be symmetrical in this case, owing to its diffuse actions of ACh (Sethuramanujam et al., 2016). Given that ACh excitation has been shown to be isotropic (Lee et al., 2010, Yonehara et al., 2011, Pei et al., 2015, Sethuramanujam et al., 2016, 2017), it was expected that the cholinergic excitation measured from SAC-ChR2 mouse line would to be acting equally along both the vertical and horizontal axes for D/V and N/T coding DSGCs (Figure 4.3). This also adds credibility to the hypothesis that BC5As are the main source of OS excitation to ON-OFF DSGCs and they further modulate the SAC output to mediate OS through SACs.

Previous studies have shown that cholinergic, GABAergic, and glutamatergic synapses are made relatively uniformly throughout the DSGC receptive field (Barlow and Levick, 1965; Taylor et al., 2000). So now looking at the presynaptic inputs to D/V and N/T coding DSGCs, we can infer that two distinct mechanisms seem to be working in tandem to shape OS in D/V vs N/T coding DSGCs. In D/V coding DSGCs, excitatory and inhibitory OS mechanisms are competing against each other and in N/T coding DSGCs, excitatory and inhibitory OS mechanisms are complementary (Figure 3.12).

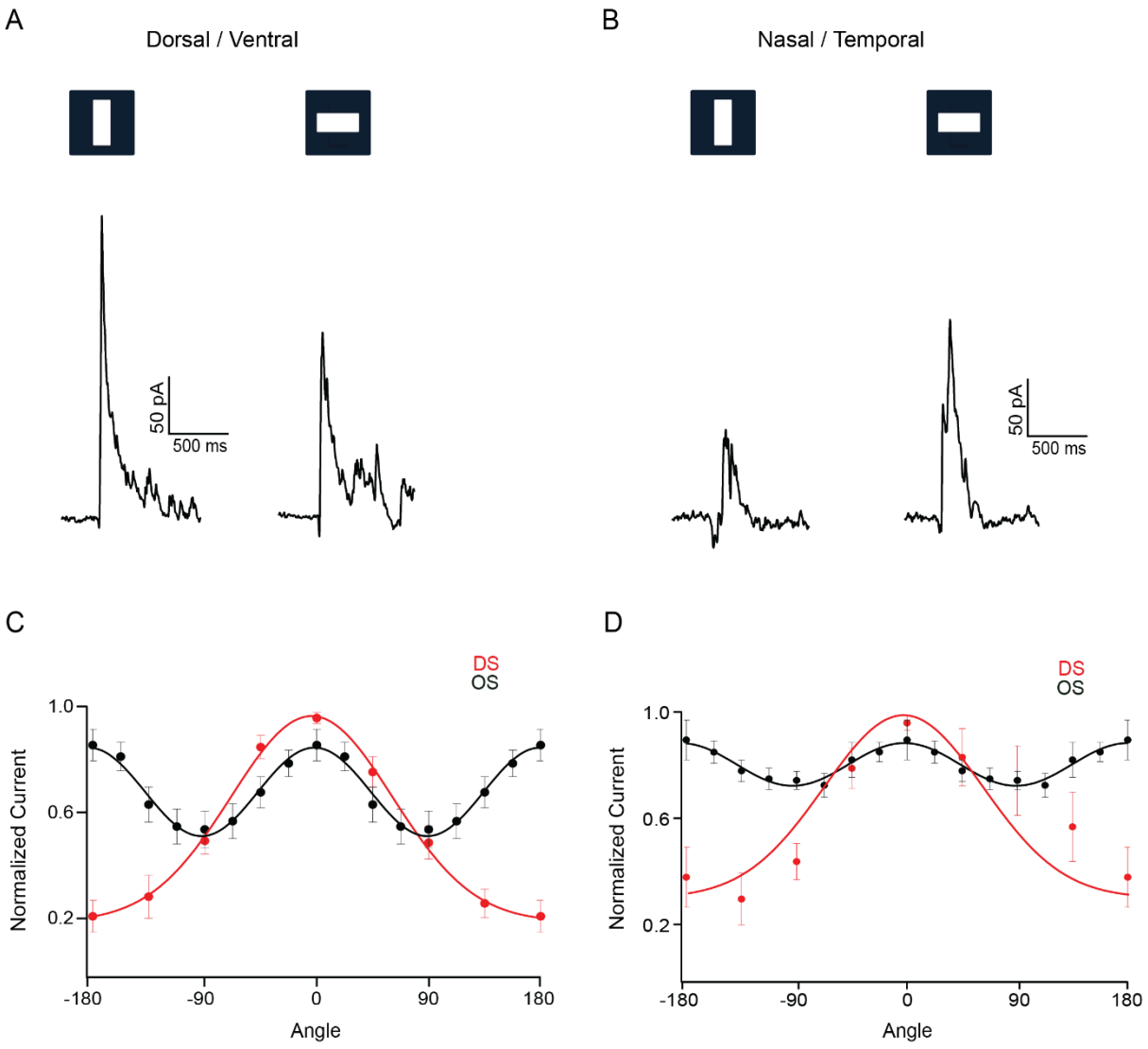

Figure 4.3 IPSC OS in D/V vs N/T coding DSGCs

(A) Sample IPSC traces obtained from a dorsal coding DSGCs for both preferred orientation (PO) and null orientation (NO) of a static bar. **(B)** Sample IPSC traces obtained from a nasal coding DSGCs for both preferred orientation (PO) and null orientation (NO) of a static bar. **(C)** Normalized IPSC tuning curves showing DS and OS tuning in dorsal/ventral coding DSGCs (n=13 cells). **(D)** Normalized IPSC tuning curves showing DS and OS tuning in nasal/temporal coding DSGCs (n=7 cells).

5. Conclusion

The pathway starting from the retina, leading to the visual cortex contains multiple layers of circuit connections that combine to extract features from the outside environment and process this information to provide form and shape photons incident on the retina. In the visual cortex, the orientation preference of DS neurons has always been strongly related to the excitatory presynaptic ensemble and weakly biased to the orientation preference of the presynaptic inhibitory partner (Rossi et al., 2020). Historically however, retinal neurons were thought to carry information about single higher order visual features (Levick, 1967; MacNeil and Masland, 1998; Baden et al., 2016). In this thesis, I have outlined how two separate features, direction and orientation are conveyed via the same output neurons and how higher order visual features are encoded by ON-OFF DSGCs. Orientation selectivity in all four types of ON-OFF DSGCs is orthogonally related to their directional tuning preference. Two distinct mechanisms, presynaptic inhibition from SACs and excitation from BC5As shape orientation selectivity in different ways. In D/V coding DSGCs, starburst inhibition dominates BC5A excitation, canceling OS glutamatergic inputs (Figure 3.5.1A). Whereas, in N/T coding DSGCs, excitatory/inhibitory OS mechanisms are complementary (Figure 3.5.1B). Overall, my work leads to novel insights about how the ON-OFF DSGCs extract OS information from the visual environment.

Studying specific circuit connections will help understand how the higher brain centers interpret the spiking pattern of DS cells and how the brain sorts out various stimulus parameters, especially during natural vision, based on the spikes it receives from a single or multiple DS cells. It has been shown that there is a strong bias for encoding vertically oriented information of natural scenes (Coppola et al., 1998). From an evolutionary standpoint, land-dwelling animals may improve their survival rate by having shorter response times to complex visual triggers from the environment. The possibility of multiple features being encoded through a single ganglion cell type is intriguing because of the potential

for parallel processing within the system. Realizing the potential advantages of one circuit pathway conveying information about two different visual features will help in deciphering how the downstream circuitry separates these components. I have explored both direction selectivity and orientation selectivity as a combined feature in the retina to aid in understanding how the central nervous system prioritizes packets of information obtained from various sensory organs.

Further experiments to understand if BC5A are the only bipolar cells tuned for vertical orientation or if the other bipolar cells providing inputs to ON-OFF DSGCs are also tuned for either vertical or horizontal orientation or are untuned needs to be conducted. This will provide a holistic view of how bipolar cells and amacrine cells work in tandem to preprocess directional information before it's transmitted to the higher brain regions for further processing. Whether similar hierarchical processing schemes exist to shape orientation and direction selectivity through an exclusive output channel and what capabilities this circuit arrangement holds in other mammalian systems remain to be tested. Utilizing this robust circuitry to study different neural networks and brain computations will also enable us to understand how various genes are responsible for stitching different pathways together. The identification of genetic markers that allow for the selective ablation of DSGCs, as well as trans-synaptic tracing to their brain targets will provide vital information regarding the contribution of these cellular structures to specific feature selectivity in higher visual centers.

6. Bibliography

Antinucci P, Abbas F, Hunter PR. 2016. Orientation selectivity in the retina: ON cell types and mechanisms. *Journal of Neuroscience* **36**:8064–8066. doi:10.1523/JNEUROSCI.1527-16.2016

Antinucci P, Hindges R. 2018. Orientation-selective retinal circuits in vertebrates. *Frontiers in Neural Circuits*, **12** (February). doi:10.3389/fncir.2018.00011

Badea TC, Nathans J. 2004. Quantitative analysis of neuronal morphologies in the mouse retina visualized by using a genetically directed reporter. *Journal of Comparative Neurology* **480**:331–351. doi:10.1002/cne.20304

Baden T, Berens P, Franke K, Román Rosón M, Bethge M, Euler T. 2016. The functional diversity of retinal ganglion cells in the mouse. *Nature* **529**:345–350. doi:10.1038/nature16468

Baldridge WH, Vaney DI, Weiler R. 1998. The modulation of intercellular coupling in the retina. *Semin Cell Dev Biol* **9**:311–318. doi:10.1006/scdb.1998.0235

Barlow, H. B., Hill, R. M. and Levick, W. R. (1964) 'Retinal ganglion cells responding selectively to direction and speed of image motion in the rabbit', J. Physiology, **173**, pp. 377–407. Available at: https://www.ncbi.nlm.nih.gov/pmc/articles/PMC1368915/pdf/jphysiol01195-0058.pdf.

Barlow, H. B. and Levick, W. R. (1965) 'The Mechanism of Directionally Selective Units', J Physiol, **178**, pp. 477–504.

Bi A, Cui J, Ma Y-P, Olshevskaya E, Pu M, Dizhoor AM, Pan Z-H. n.d. Ectopic Expression of a Microbial-Type Rhodopsin Restores Visual Responses in Mice with Photoreceptor Degeneration. Neuron. 2006 April 6; **50(1)**: 23–33.

Bloomfield, S. A. (1991) 'Two types of orientation-sensitive responses of amacrine cells in the mammalian retina', Nature, 350, pp. 347–350.

Bloomfield SA. 1994. Orientation-Sensitive Amacrine and Ganglion Cells in the Rabbit Retina, Journal of Neurophysiology, **71(5)**, pp. 1672–1691. doi: 10.1152/jn.1994.71.5.1672.

Borst A, Euler T (2011) Seeing Things in Motion: Models, Circuits, and Mechanisms. Neuron 71:974-994.

Briggman KL, Helmstaedter M, Denk W. 2011. Wiring specificity in the direction-selectivity circuit of the retina. *Nature* **471**:183–190. doi:10.1038/nature09818

Chen H, Liu X, Tian N. 2014. Subtype-dependent postnatal development of direction-and orientation-selective retinal ganglion cells in mice. *J Neurophysiol* **112**:2092–2101. doi:10.1152/jn.00320.2014.-The

Chiao CC, Masland RH. 2003. Contextual tuning of direction-selective retinal ganglion cells. *Nat Neurosci* **6**:1251–1252. doi:10.1038/nn1147

Chiao C-C, Masland RH. 2002. Brief Communication Starburst Cells Nondirectionally Facilitate the Responses of Direction-Selective Retinal Ganglion Cells.

Coppola DM, Purves HR, Mccoy AN, Purves D. 1998. The distribution of oriented contours in the real world, PNAS, **95(7)**, pp. 4002–4006. doi: 10.1073/pnas.95.7.4002

Cruz-Martín A, El-Danaf RN, Osakada F, Sriram B, Dhande OS, Nguyen PL, Callaway EM, Ghosh A, Huberman AD. 2014. A dedicated circuit links direction-selective retinal ganglion cells to the primary visual cortex. *Nature* **507**:358–361. doi:10.1038/nature12989

Demb JB, Haarsma L, Freed MA, Sterling P (1999) Functional circuitry of the retinal ganglion cell's nonlinear receptive field. J Neurosci 19:9756-9767.

Demb JB, Singer JH. 2012. Intrinsic properties and functional circuitry of the AII amacrine cell. *Vis Neurosci*. doi:10.1017/S0952523811000368

Demb JB, Singer JH (2015) Functional Circuitry of the Retina. Annual Review of Vision Science 1:263-289.

Ding H, Smith RG, Poleg-Polsky A, Diamond JS, Briggman KL. 2016. Species-specific wiring for direction selectivity in the mammalian retina. *Nature* **535**:105–110. doi:10.1038/nature18609

Duan X, Krishnaswamy A, de La Huerta I, Sanes JR. 2014. Type II cadherins guide assembly of a direction-selective retinal circuit. *Cell* **158**:793–807. doi:10.1016/j.cell.2014.06.047

Dowling, J. E. (1987). The retina: an approachable part of the brain. Cambridge, Mass: Belknap Press of Harvard University Press.

Euler T, Masland RH. 2000. Light-Evoked Responses of Bipolar Cells in a Mammalian Retina. Journal of Neurophysiology, 83(4), pp. 1817–1829. doi: 10.1152/jn.2000.83.4.1817.

Farrow K, Teixeira M, Szikra T, Viney TJ, Balint K, Yonehara K, Roska B. 2013. Ambient illumination toggles a neuronal circuit switch in the retina and visual perception at cone threshold. *Neuron* **78**:325–338. doi:10.1016/j.neuron.2013.02.014

Feller MB, Chen Q, Pei Z, Koren D, Wei W. 2016. Stimulus-dependent recruitment of lateral inhibition underlies retinal direction selectivity. doi:10.7554/eLife.21053.001

Fiscella M, Felix Franke X, Farrow K, Müller J, Roska B, Azeredo da Silveira R, Hierlemann A. 2015. Visual coding with a population of direction-selective neurons. *J Neurophysiol* **114**:2485–2499. doi:10.1152/jn.00919.2014.

Fisher YE, Silies M, Clandinin TR. 2015. Orientation Selectivity Sharpens Motion Detection in Drosophila. *Neuron* **88**:390–402. doi:10.1016/j.neuron.2015.09.033

Franke K, Berens P, Schubert T, Bethge M, Euler T, Baden T. 2017. Inhibition decorrelates visual feature representations in the inner retina. *Nature* **542**:439–444. doi:10.1038/nature21394

Fransen JW, Borghuis BG. 2017. Temporally Diverse Excitation Generates Direction-Selective Responses in ON- and OFF-Type Retinal Starburst Amacrine Cells. *Cell Rep* **18**:1356–1365. doi:10.1016/j.celrep.2017.01.026

Freeman AW. 2021. A model for the origin of motion direction selectivity in visual cortex. *Journal of Neuroscience* **41**:89–102. doi:10.1523/JNeurosci.1362-20.2020

Fried SI, Mü nch TA, Werblin FS. 2002. Mechanisms and circuitry underlying directional selectivity in the retina. pp. **411**–414.

Fukuda T, Kosaka T. 2000. Gap Junctions Linking the Dendritic Network of GABAergic Interneurons in the Hippocampus. The Journal of Neuroscience, February 15, 2000, **20(4)**:1519–1528

Girshick AR, Landy MS, Simoncelli EP. 2011. Cardinal rules: Visual orientation perception reflects knowledge of environmental statistics. *Nat Neurosci* **14**:926–932. doi:10.1038/nn.2831

Grzywacz NM, Merwine DK, Amthor FR. 1998. Complementary roles of two excitatory pathways in retinal directional selectivity. *Vis Neurosci* **15**:1119–1127. doi:10.1017/S0952523898156109

Grzywacz NM, Tootle JS, Amthor FR. 1997. Is the input to a GABAergic or cholinergic synapse the sole asymmetry in rabbit's retinal directional selectivity? *Vis Neurosci* **14**:39–54. doi:10.1017/S0952523800008749

Hanson L, Ravi-Chander P, Berson D, Awatramani GB. 2023. Hierarchical retinal computations rely on hybrid chemical-electrical signaling. *Cell Rep* **42**:112030. doi:10.1016/j.celrep.2023.112030

Hanson L, Sethuramanujam S, Derosenroll G, Jain V, Awatramani GB. 2019. Retinal direction selectivity in the absence of asymmetric starburst amacrine cell responses. doi:10.7554/eLife.42392.001

He, S., Levick, W. R. and Vaney, D. I. (1998) 'Distinguishing direction selectivity from orientation selectivity in the rabbit retina.', Visual neuroscience. University of Victoria Libraries, **15(3)**, pp. 439–47. doi: 10.1017/S0952523898153038.

Heidelberger, R., Thoreson, W. B. and Witkovsky, P. (2005) 'Synaptic transmission at retinal ribbon synapses', Progress in Retinal and Eye Research, **24(6)**, pp. 682–720. doi: 10.1016/j.preteyeres.2005.04.002.

Helmstaedter M, Briggman KL, Turaga SC, Jain V, Seung HS, Denk W. 2013. Connectomic reconstruction of the inner plexiform layer in the mouse retina. *Nature* **500**:168–174. doi:10.1038/nature12346.

Henry G.H, Bishop P.O., Dreher B. 1974. Orientation axis and direction as stimulus parameters for striate cells. Vision Res. Vol. **14**. pp. 767-777. Pergamon Press 1974.

Hoggarth A, McLaughlin AJ, Ronellenfitch K, Trenholm S, Vasandani R, Sethuramanujam S, Schwab D, Briggman KL, Awatramani GB. 2015. Specific wiring of distinct amacrine cells in the directionally selective retinal circuit permits independent coding of direction and size. *Neuron* **86**:276–291. doi:10.1016/j.neuron.2015.02.035

Huang X, Rangel M, Briggman KL, Wei W. 2019. Neural mechanisms of contextual modulation in the retinal direction selective circuit. *Nat Commun* **10**. doi:10.1038/s41467-019-10268-z

Hubel, D. H. and Wiesel, A. T. N. (1962) Receptive fields, binocular interaction and functional architecture in the Cat's visual cortex, J. Phyisiol.

Hubel, D. H. and Wiesel, T. N. (1959) 'Receptive Fields of Single Neurones in the Cat's Striate Cortex', J. Physiology, **148**, pp. 574–591.

Jain V, Murphy-Baum BL, Derosenroll G, Sethuramanujam S, Delsey M, Delaney K, Awatramani GB. The functional organization of excitation and inhibition in the dendrites of mouse direction-selective ganglion cells.

Jarsky T, Cembrowski M, Logan SM, Kath WL, Riecke H, Demb JB, Singer JH. 2011. A synaptic mechanism for retinal adaptation to luminance and contrast. *Journal of Neuroscience* **31**:11003–11015. doi:10.1523/JNEUROSCI.2631-11.2011

Jin Kim Y, Peterson B, Crook J, Joo H, Wu J, Puller C, Robinson F, Gamlin P, Yau K-W, Viana Universidad Miguel Hernandez John Troy F, Smith R, Packer O, Detwiler P, Dacey D. n.d. Origins of direction selectivity in the primate retina. doi:10.21203/rs.3.rs-1059762/v1

Johnston J, Seibel SH, Darnet LSA, Renninger S, Orger M, Lagnado L. 2019a. A Retinal Circuit Generating a Dynamic Predictive Code for Oriented Features. *Neuron* **102**:1211-1222.e3. doi:10.1016/j.neuron.2019.04.002

Kim JS, Greene MJ, Zlateski A, Lee K, Richardson M, Turaga SC, Purcaro M, Balkam M, Robinson A, Behabadi BF, Campos M, Denk W, Seung HS. 2014. Space-time wiring specificity supports direction selectivity in the retina. *Nature* **509**:331–336. doi:10.1038/nature13240

Kim T, Freeman RD. 2016. Direction selectivity of neurons in the visual cortex is non-linear and lamina-dependent. *European Journal of Neuroscience* **43**:1389–1399. doi:10.1111/ejn.13223

Kolb H (1974) The connections between horizontal cells and photoreceptors in the retina of the cat: electron microscopy of Golgi preparations. J Comp Neurol 155:1-14.

Kolb H (2003) How the retina works. American scientist 91:28-35.

Lagali, P., Balya, D., Awatramani, G. et al. Light-activated channels targeted to ON bipolar cells restore visual function in retinal degeneration. Nat Neurosci 11, 667–675 (2008). https://doi.org/10.1038/nn.2117

Lee S, Kim K, Zhou ZJ. 2010. Role of ACh-GABA Cotransmission in Detecting Image Motion and Motion Direction. *Neuron* **68**:1159–1172. doi:10.1016/j.neuron.2010.11.031

Lee S, Zhou ZJ. 2006. The Synaptic Mechanism of Direction Selectivity in Distal Processes of Starburst Amacrine Cells. *Neuron* **51**:787–799. doi:10.1016/j.neuron.2006.08.007

Lee SCS, Meyer A, Schubert T, Hüser L, Dedek K, Haverkamp S. 2015. Morphology and connectivity of the small bistratified A8 amacrine cell in the mouse retina. *Journal of Comparative Neurology* **523**:1529–1547. doi:10.1002/cne.23752

Levick, W. R. (1967) 'Receptive fields and trigger features of ganglion cells in the visual streak of the Rabbit's retina', J. Physiol, 188, pp. 285–307

Li, Y.-T. et al. (2015) 'Strengthening of Direction Selectivity by Broadly Tuned and Spatiotemporally Slightly Offset Inhibition in Mouse Visual Cortex', cerebral cortex, 25(9), pp. 2466–2477. doi: 10.1093/cercor/bhu049.

Lien AD, Scanziani M. 2018. Cortical direction selectivity emerges at convergence of thalamic synapses. *Nature* **558**:80–86. doi:10.1038/s41586-018-0148-5

MacNeil MA, Masland RH (1998) Extreme diversity among amacrine cells: implications for function. Neuron 20:971-982.

Masland, R. H. (2001) 'The fundamental plan of the retina', Nature Neuroscience, 4(9), pp. 877– 886. Available at: http://neurosci.nature.com.

Masland RH. 2012. The Neuronal Organization of the Retina. *Neuron*. doi: 10.1016/j.neuron.2012.10.002

Matsumoto A, Briggman KL, Yonehara K. 2019. Spatiotemporally Asymmetric Excitation Supports Mammalian Retinal Motion Sensitivity. *Current Biology* **29**:3277-3288.e5. doi:10.1016/j.cub.2019.08.048

Mauss AS, Vlasits A, Borst A, Feller M. 2017. Visual Circuits for Direction Selectivity. *Annu Rev Neurosci* **40**:211–230. doi:10.1146/annurev-neuro-072116-031335

Mayer, M. L., Westbrook, G. L. and Guthrie, P. B. (1984) 'Voltage-dependent block by Mg2+ of NMDA responses in spinal cord neurones', Nature, 309, pp. 261–263

Münch TA, Werblin FS. 2006. Symmetric interactions within a homogeneous starburst cell network can lead to robust asymmetries in dendrites of starburst amacrine cells. *J Neurophysiol* **96**:471–477. doi:10.1152/jn.00628.2005

Murphy-Baum BL, Awatramani GB. 2022. Parallel processing in active dendrites during periods of intense spiking activity. *Cell Rep* **38**. doi:10.1016/j.celrep.2022.110412

Murphy-Baum BL, Rowland Taylor W. 2015. The synaptic and morphological basis of orientation selectivity in a polyaxonal amacrine cell of the rabbit retina. *Journal of Neuroscience* **35**:13336–13350. doi:10.1523/JNEUROSCI.1712-15.2015

Nagel G, Szellas T, Huhn W, Kateriya S, Adeishvili N, Berthold P, Ollig D, Hegemann P, Bamberg E. Channelrhodopsin-2, a directly light-gated cation-selective membrane channel. Proc Natl Acad Sci U S A. 2003 Nov 25;100(24):13940-5. doi: 10.1073/pnas.1936192100. Epub 2003 Nov 13. PMID: 14615590; PMCID: PMC283525.

Nath, A. and Schwartz, G. W. (2016) 'Cardinal Orientation Selectivity Is Represented by Two Distinct Ganglion Cell Types in Mouse Retina.', The Journal of neuroscience : the official journal of the Society for Neuroscience, 36(11), pp. 3208–21. doi: 10.1523/JNEUROSCI.4554- 15.2016.

Nath, A. and Schwartz, G. W. (2017) 'Electrical synapses convey orientation selectivity in the mouse retina', Nature communications. Springer US, 8(1), p. 2025. doi: 10.1038/s41467-017- 109 01980-9.

Oesch N, Euler T, Taylor WR. 2005. Direction-selective dendritic action potentials in rabbit retina. *Neuron* **47**:739–750. doi:10.1016/j.neuron.2005.06.036

O'malley DM, Masland RH. 1989. Co-release of acetylcholine and y-aminobutyric acid by a retinal neuron (retina/amacrine cell/neurotransmitter/colocalization), Proc. Nati. Acad. Sci. USA.

Oyster, C. W. and Barlow, H. B. (1967) 'Direction-Selective Units in Rabbit Retina : Distribution of Preferred Directions Published by : American Association for the Advancement of Science Stable URL : https://www.jstor.org/stable/1720260 REFERENCES Linked references are available on JSTOR for ', 155(3764), pp. 841–842.

Park S. J. H., Kim IJ, Looger LL, Demb JB, Borghuis BG. 2014. Excitatory synaptic inputs to mouse on-off direction- selective retinal ganglion cells lack direction tuning. *Journal of Neuroscience* **34**:3976–3981. doi:10.1523/JNEUROSCI.5017-13.2014

Passaglia CL, Troy JB, Ruttiger L, Lee BB. n.d. Orientation sensitivity of ganglion cells in primate retina, Vision Research **42** (2002) 683–694

Poleg-Polsky, A. and Diamond, J. S. (2011) 'Imperfect Space Clamp Permits Electrotonic Interactions between Inhibitory and Excitatory Synaptic Conductances, Distorting Voltage Clamp Recordings', PLoS ONE, **6(4)**, p. 19463. doi: 10.1371/journal.pone.0019463.

Poleg-Polsky, A. and Diamond, J. S. (2016) 'Retinal circuitry balances contrast tuning of excitation and inhibition to enable reliable computation of direction selectivity', Journal of Neuroscience, **36(21)**, pp. 5861–5876. doi: 10.1523/JNEUROSCI.4013-15.2016.

Poleg-Polsky, A., Ding, H. and Diamond, J. S. (2018) 'Functional Compartmentalization within Starburst Amacrine Cell Dendrites in the Retina', Cell Reports. ElsevierCompany., **22(11)**, pp. 2809–2817. doi: 10.1016/j.celrep.2018.02.064.

Priebe NJ, Cassanello CR, Lisberger SG (2003) The neural representation of speed in macaque area MT/V5. J Neurosci 23:5650-5661.

Priebe NJ, Ferster D (2008) Inhibition, spike threshold, and stimulus selectivity in primary visual cortex. Neuron 57:482-497.

Raviola E, Gilula NB. 1973. Gap Junctions between Photoreceptor Cells in the Vertebrate Retina (membranes/electron microscopy/freeze-fracturing).

Rieke, F. and Rudd, M. E. (2009) 'The Challenges Natural Images Pose for Visual Adaptation', Neuron. Elsevier Inc., **64(5)**, pp. 605–616. doi: 10.1016/j.neuron.2009.11.028.

Rivlin-Etzion, M. et al. (2011) 'Transgenic mice reveal unexpected diversity of On-Off direction selective retinal ganglion cell subtypes and brain structures involved in motion processing', J Neurosci, **31(24)**, pp. 8760–8769. doi: 10.1523/JNEUROSCI.0564-11.2011.Transgenic.

Rivlin-Etzion, M., Wei, W. and Feller, M. B. (2012) 'Visual Stimulation Reverses the Directional Preference of Direction-Selective Retinal Ganglion Cells', Neuron. Elsevier Inc., **76(3)**, pp. 518–525. doi: 10.1016/j.neuron.2012.08.041

Roy, S. and Field, G. D. (2019) 'Dopaminergic modulation of retinal processing from starlight to sunlight', Journal of Pharmacological Science. Elsevier Ltd, **140(1)**, pp. 86–93. doi: 10.1016/j.jphs.2019.03.006.

Rudolph, S. et al. (2015) 'The ubiquitous nature of multivesicular release', Trends in Neurosciences. Elsevier Ltd, **38(7)**, pp. 428–438. doi: 10.1016/j.tins.2015.05.008.

Saul AB, Carras PL, Humphrey AL. 2005. Temporal properties of inputs to direction-selective neurons in monkey V1. *J Neurophysiol* **94**:282–294. doi:10.1152/jn.00868.2004

Saul AB, Feidler JC. 2002. Development of Response Timing and Direction Selectivity in Cat Visual Thalamus and Cortex.

Saul AB, Humphrey AL. 1990. Spatial and Temporal Response Properties of Lagged and Nonlagged Cells in Cat Lateral Geniculate Nucleus, Journal of Neurophysiology.

Schachter MJ, Oesch N, Smith RG, Rowland Taylor W. 2010. Dendritic spikes amplify the synaptic signal to enhance detection of motion in a simulation of the direction-selective ganglion cell. *PLoS Comput Biol* **6**. doi:10.1371/journal.pcbi.1000899

Sethuramanujam S, Awatramani GB, Slaughter MM. 2018. Cholinergic excitation complements glutamate in coding visual information in retinal ganglion cells. *Journal of Physiology* **596**:3709–3724. doi:10.1113/JP275073

Sethuramanujam S, Matsumoto A, deRosenroll G, Murphy-Baum B, McIntosh JM, Jing M, Li Y, Berson D, Yonehara K, Awatramani GB. 2021. Rapid multi-directed cholinergic transmission in the central nervous system. *Nat Commun* **12**. doi: 10.1038/s41467-021-21680-9

Sethuramanujam S, McLaughlin AJ, deRosenroll G, Hoggarth A, Schwab DJ, Awatramani GB. 2016. A Central Role for Mixed Acetylcholine/GABA Transmission in Direction Coding in the Retina. *Neuron* **90**:1243–1256. doi:10.1016/j.neuron.2016.04.041

Sethuramanujam S, Yao X, deRosenroll G, Briggman KL, Field GD, Awatramani GB. 2017. "Silent" NMDA Synapses Enhance Motion Sensitivity in a Mature Retinal Circuit. *Neuron* **96**:1099-1111.e3. doi:10.1016/j.neuron.2017.09.058

Shapley R, Hawken M, Ringach DL, McLaughlin by, collabo- their. 2003. Review Dynamics of Orientation Selectivity in the Primary Visual Cortex and the Importance of Cortical Inhibition mental work and also on recent theoretical work and modeling, Neuron.

Shekhar K, Lapan SW, Whitney IE, Tran NM, Macosko EZ, Kowalczyk M, Adiconis X, Levin JZ, Nemesh J, Goldman M, McCarroll SA, Cepko CL, Regev A, Sanes JR. 2016. Comprehensive Classification of Retinal Bipolar Neurons by Single-Cell Transcriptomics. *Cell* **166**:1308-1323.e30. doi:10.1016/j.cell.2016.07.054

Shigang HE, Levick WR, Vaney DI. 1998. Distinguishing direction selectivity from orientation selectivity in the rabbit retina. *Vis Neurosci* **15**:439–447. doi:10.1017/S0952523898153038

Singer JH. 2007. Multivesicular release and saturation of glutamatergic signalling at retinal ribbon synapses. *Journal of Physiology*. doi:10.1113/jphysiol.2006.125302

Sivyer, B. et al. (2010) 'Synaptic inputs and timing underlying the velocity tuning of directionselective ganglion cells in rabbit retina', J Physiol, 588, pp. 3243–3253. doi: 10.1113/jphysiol.2010.192716.

Sivyer, B. and Williams, S. R. (2013) 'Direction selectivity is computed by active dendritic integration in retinal ganglion cells', Nature Publishing Group, 16(8). doi: 10.1038/nn.3565.

Stabio ME, Sondereker KB, Haghgou SD, Day BL, Chidsey B, Sabbah S, Renna JM. 2018. A novel map of the mouse eye for orienting retinal topography in anatomical space. *Journal of Comparative Neurology* **526**:1749–1759. doi:10.1002/cne.24446

Summers MT, Feller MB. 2022. Distinct inhibitory pathways control velocity and directional tuning in the mouse retina. *Current Biology* **32**:2130-2143.e3. doi:10.1016/j.cub.2022.03.054

Sun W, Tan Z, Mensh BD, Ji N. 2016. Thalamus provides layer 4 of primary visual cortex with orientation- and direction-tuned inputs. *Nat Neurosci* **19**:308–315. doi:10.1038/nn.4196

Taylor, W. R. et al. (2000) 'Dendritic computation of direction selectivity by retinal ganglion cells', Science, **289**(5488), pp. 2347–2350. doi: 10.1126/science.289.5488.2347.

Taylor WR, Vaney DI. 2002. Diverse Synaptic Mechanisms Generate Direction Selectivity in the Rabbit Retina, The Journal of Neuroscience.

Taylor WR, Smith RG. 2012. The role of starburst amacrine cells in visual signal processing. *Vis Neurosci* **29**:73–81. doi:10.1017/S0952523811000393

Thiele, A. et al. (2004) ‘Contribution of inhibitory mechanisms to direction selectivity and response normalization in macaque middle temporal area’, PNAS, **101(26)**, pp. 9810–9815. Available at: www.pnas.orgcgidoi10.1073pnas.0307754101.

Torre, V. and Poggio, T. (1978) ‘A synaptic mechanism possibly underlying directional selectivity to motion’, Proc. R. Soc. Lond., **202**, pp. 409–416. Available at: https://royalsocietypublishing.org/.

Trenholm, S. et al. (2013) ‘Lag normalization in an electrically coupled neural network’, Nature Neuroscience, 16(2), pp. 154–156. doi: 10.1038/nn.3308.

Trenholm, S. et al. (2014) ‘Nonlinear dendritic integration of electrical and chemical synaptic inputs drives fine-scale correlations’, Nature Neuroscience. Nature Publishing Group, 17(12), pp. 1759–1766. doi: 10.1038/nn.3851.

Tsukamoto Y, Omi N. 2017. Classification of mouse retinal bipolar cells: Type-specific connectivity with special reference to rod-driven AII amacrine pathways. *Front Neuroanat* **11**. doi:10.3389/fnana.2017.00092

Tukker JJ, Taylor WR, Smith RG. 2004. Direction selectivity in a model of the starburst amacrine cell. *Vis Neurosci* **21**:611–625. doi:10.1017/S0952523804214109

Vaney DI, Sivyer B, Taylor WR. 2012. Direction selectivity in the retina: Symmetry and asymmetry in structure and function. *Nat Rev Neurosci*. doi:10.1038/nrn3165

Venkataramani S, Taylor WR. 2010. Orientation selectivity in rabbit retinal ganglion cells is mediated by presynaptic inhibition. *Journal of Neuroscience* **30**:15664–15676. doi:10.1523/JNeurosci.2081-10.2010

Venkataramani S, Taylor WR. 2016. Synaptic mechanisms generating orientation selectivity in the on pathway of the rabbit retina. *Journal of Neuroscience* **36**:3336–3349. doi:10.1523/JNeurosci.1432-15.2016

Vlasits AL, Bos R, Morrie RD, Fortuny C, Flannery JG, Feller MB, Rivlin-Etzion M. 2014. Visual Stimulation Switches the Polarity of Excitatory Input to Starburst Amacrine Cells. *Neuron* **83**:1172–1184. doi:10.1016/j.neuron.2014.07.037

Vlasits AL, Morrie RD, Tran-Van-Minh A, Bleckert A, Gainer CF, DiGregorio DA, Feller MB. 2016. A Role for Synaptic Input Distribution in a Dendritic Computation of Motion Direction in the Retina. *Neuron* **89**:1317–1330. doi:10.1016/j.neuron.2016.02.020

Völgyl B, Chheda S, Bloomfield SA. 2009. Tracer coupling patterns of the ganglion cell subtypes in the mouse retina. *Journal of Comparative Neurology* **512**:664–687. doi:10.1002/cne.21912

Völgyi B, Kovács-öller T, Atlasz T, Wilhelm M, Gábriel R. 2013. Gap junctional coupling in the vertebrate retina: Variations on one theme? *Prog Retin Eye Res*. doi:10.1016/j.preteyeres.2012.12.002

Wilent WB, Contreras D. 2005. Dynamics of excitation and inhibition underlying stimulus selectivity in rat somatosensory cortex. *Nat Neurosci* **8**:1364–1370. doi:10.1038/nn1545

Wilson DE, Scholl B, Fitzpatrick D. 2018. Differential tuning of excitation and inhibition shapes direction selectivity in ferret visual cortex. *Nature* **560**:97–101. doi:10.1038/s41586-018-0354-1

Yan W, Laboulaye MA, Tran NM, Whitney IE, Benhar I, Sanes JR. 2020. Mouse Retinal Cell Atlas: Molecular Identification of over Sixty Amacrine Cell Types. *Journal of Neuroscience* **40**:5177–5195. doi:10.1523/JNEUROSCI.0471-20.2020

Yang, G. and Masland, R. H. (1992) 'Direct Visualization of the Dendritic and Receptive Fields of Directionally Selective Retinal Ganglion Cells', Science, 258(5090), pp. 1949–1952.

Yang G, Masland RH. 1994. Receptive Fields and Dendritic Structure of Directionally Selective Retinal Ganglion Cells, The Journal of Neuroscience.

Yao X, Cafaro J, McLaughlin AJ, Postma FR, Paul DL, Awatramani G, Field GD. 2018. Gap Junctions Contribute to Differential Light Adaptation across Direction-Selective Retinal Ganglion Cells. *Neuron* **100**:216-228.e6. doi:10.1016/j.neuron.2018.08.021

Yonehara K, Balint K, Noda M, Nagel G, Bamberg E, Roska B. 2011. Spatially asymmetric reorganization of inhibition establishes a motion-sensitive circuit. *Nature* **469**:407–410. doi:10.1038/nature09711

Yonehara K, Farrow K, Ghanem A, Hillier D, Balint K, Teixeira M, Jüttner J, Noda M, Neve RL, Conzelmann KK, Roska B. 2013. The first stage of cardinal direction selectivity is localized to the dendrites of retinal ganglion cells. *Neuron* **79**:1078–1085. doi:10.1016/j.neuron.2013.08.005

Yoshida K, Watanabe D, Ishikane H, Tachibana M, Pastan I, Nakanishi S. 2001. A Key Role of Starburst Amacrine Cells in Originating Retinal Directional Selectivity and Optokinetic Eye Movement, Neuron.

Zhang, A.-J. and Wu, S. M. (2009) 'Behavioral/Systems/Cognitive Receptive Fields of Retinal Bipolar Cells Are Mediated by Heterogeneous Synaptic Circuitry'. doi: 10.1523/JNeurosci.4984-08.2009.

Zhao, X. et al. (2013) 'Orientation-selective responses in the mouse lateral geniculate nucleus', Journal of Neuroscience, 33(31), pp. 12751–12763. doi: 10.1523/JNeurosci.0095-13.2013.

7. Appendix

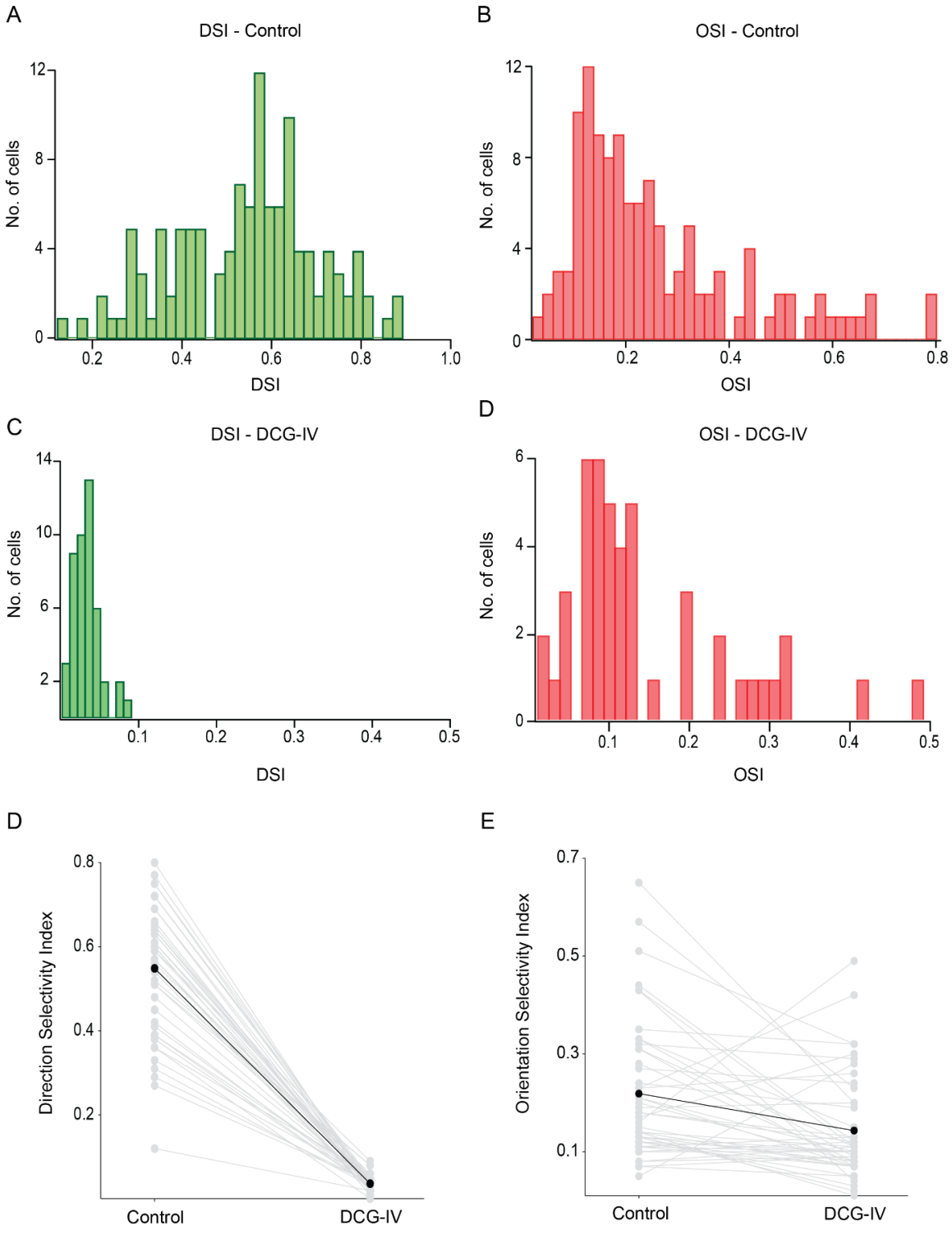
A
DSI - Control
No. of cells
DSI
B
OSI - Control
No. of cells
OSI
C
DSI - DCG-IV
No. of cells
DSI
D
OSI - DCG-IV
No. of cells
OSI
D
Direction Selectivity Index
Control
DCG-IV
E
Orientation Selectivity Index
Control
DCG-IV

Appendix 1 – DSI/OSI measurements in control vs DCG-IV conditions

(A) Histogram of DSI across the population calculated as the vector sum of responses from bars moving in 8 different directions (n=117 cells) under control conditions. **(B)** Histogram of OSI across the population calculated as the vector sum of responses from static bars flashing in 8 orientations (n=117 cells) under control conditions. **(C)** Histogram of DSI across the population calculated as the vector sum of responses from bars moving in 8 different directions (n=46 cells) under DCG-IV conditions. **(D)** Histogram of OSI across the population calculated as the vector sum of responses from static bars flashing in 8 orientations (n=46 cells) under DCG-IV conditions. **(E)** Paired plots constructed from DSI values obtained from ON-OFF DSGCs in control vs DCG-IV conditions. **(F)** Paired plots constructed from OSI values obtained from ON-OFF DSGCs in control vs DCG-IV conditions. (DSI – Direction selectivity index; OSI – Orientation selectivity index).